CHAPTER IV
RESULTS AND DISCUSSION

4.1 Microemulsion Formation with Crude Palm Oil

The most desirable property of surfactant used for residual oil extraction is the ability to reduce sufficiently IFT between oil retained in SBE and surfactant solution resulting in detachment of oil droplet from SBE surface. The middle phase microemulsion (Winsor type III) is applicable for residual oil extraction. The surfactant formulation at type III microemulsion can effectively produce an ultralow IFT (<0.1 mN/m) with high oil solubilization capacity at a small amount of surfactant concentration. Another important parameter affecting the oil removal from SBE is the surfactant type. As the SBE's surface is net negatively charge, anionic extended and nonionic surfactant system were selected, alcohol ethoxylated surfactant ($C_{12,14}$-$(EO)_n$-OH, n=3,9) and sodium alkyl propoxylated sulfate ($C_{12,13}$-$(PO)_n$-SO_4Na, n=4,8), respectively. The anionic extended surfactants were selected because they have been proven to reduce the IFT and provided high solubilization capacity with high hydrophobic oils, e.g., triglyceride and vegetable oil (Phan *et al.*, 2010). The nonionic surfactants were selected in this work due to the fact that they can form microemuslion without addition of salt. An additional point is that both of these surfactant types can reduce the losses from surfactant adsorption due to the charge interaction of the surfactant's head and SBE surface. Therefore, all surfactant systems were evaluated based on their structure and micellar properties at oil-water and air-water interfaces.

4.1.1 Correlation between Surfactant Structure and their Properties

The surfactants used in this study contain different head group and different extended parts either polyethylene oxide (EO) or polypropylene oxide (PO) group inserted between hydrophilic and hydrophobic part. Table 4.1 shows the properties of the surfactants used in this study. The critical micelle concentration (CMC), surface excess concentration (Γ) and surface area per molecule (A_{min}) values were calculated from surface tension (γ) measurement at temperature of 25 ± 2 °C.

The CMC values were determined from the intersection of two linear derived from relation between surface tension (mN/m) and surfactant concentration (log). Furthermore, the adsorption of surfactant molecule at the liquid and air interfaces was calculated based on Gibbs adsorption equation (Mukherjee *et al.*, 2013).

Table 4.1 Hydrophilic-lipophilic balance (HLB), critical micelle concentration (CMC), surface excess concentration (Γ), and area per molecule (A_{min}) of nonionic and anionic extended surfactants

Surfactant	HLB[a]	CMC (mM)	Slope		Γ[c] (mmol/1000m^2)	A_{min}[c] (Å^2)
			Slope[b]	r^2		
$C_{12,14}H_{25,29}$–$(EO)_3$–OH	7.98	0.036	-11.7	0.997	2.051	81
$C_{12,14}H_{25,29}$–$(EO)_9$–OH	13.31	0.045	-8.174	0.996	1.433	116
$C_{12,13}H_{25,27}$–$(PO)_4$–SO_4Na	38.26	0.099	-7.047	0.996	0.618	269
$C_{12,13}H_{25,27}$–$(PO)_8$–SO_4Na	37.66	0.142	-6.807	0.997	0.596	278

Notes

[a] HLB is calculated based on equation (A.1) and (A.2)

[b] From Figure A1 – A4.

[c] Γ and A_{min} is obtained equation (A.3) and (A.4)

4.1.1.1 Hydrophilic-Lipophilic Balance (HLB)

The hydrophobicity of surfactant molecule is often characterized by hydrophilic-lipophilic balance or HLB. HLB indicates a good solubility in polar such as water (high HLB) or non-polar system such as oil (low HLB). As seen in Table 4.1, the HLB values of both anionic extended surfactants are relatively higher than those of nonionic surfactants. In the other word, higher HLB value presents more favorable water phase of surfactant. It is indicated that the sulfate head group has a stronger interaction with water even if their structure contain PO molecules, which are able to increase hydrophobicity of the tail further without reducing water solubility. The fact that $C_{12,13}H_{25,27}$–$(PO)_4$–SO_4Na and $C_{12,13}H_{25,27}$–$(PO)_8$–SO_4Na contain 4-PO and 8-PO groups inserted between head and tail region,

respectively. It can be concluded that the anionic extended surfactants had a unique characteristic. They not only can increase the oil solubilization capacity but also can provide more water interaction. For nonionic surfactant systems, the nonionic surfactant with 9-EO groups had greater HLB value compared to those 3-EO groups. The EO molecules acted as an extended part in nonionic head group, they enhanced interaction with water side or hydrophilic part and gave a smooth phase transition at interface (Phan *et al.*, 2011). The structures of PO and EO groups are illustrated in Figure 4.1.

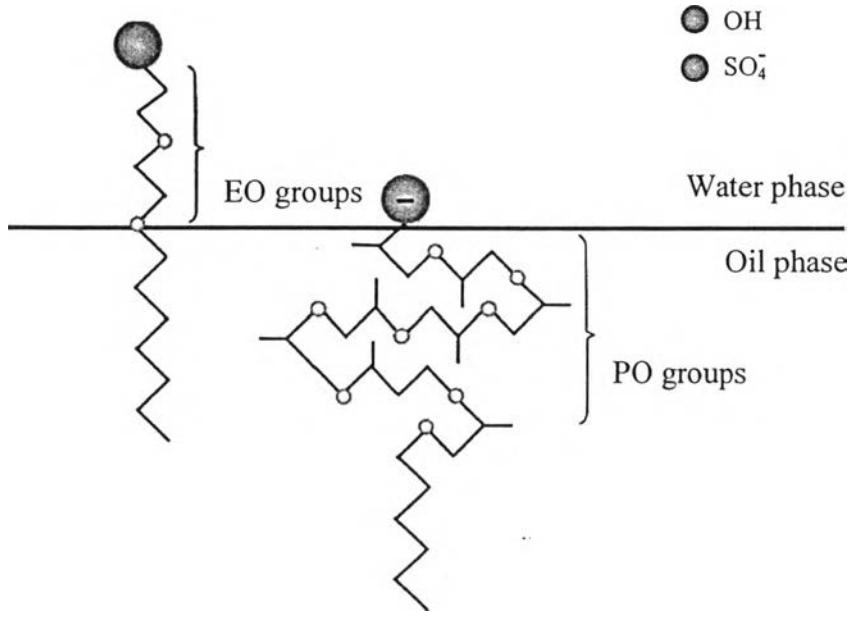

Figure 4.1 Schematic molecular structure of polyethylene oxide (EO) and polypropylene oxide (PO) groups inserted between hydrophilic and hydrophobic part of the surfactant.

4.1.1.2 Critical Micelle Concentration (CMC)

The CMC of the surfactant is the value at which monomers are first to form self-aggregate to be a micelle. The most common method for measuring CMC is determined through surface tension measurement. All surfactant systems used were varied by surfactant concentration with no adding salt. The transition point between two linear lines is used to determine the CMC of the surfactant system

(Charoensaeng *et al.*, 2008). The CMCs of each surfactant used in this study are shown in Figure 4.2. For nonionic alcohol ethoxylated surfactant system, increasing the EO groups in hydrophilic part caused an increase in the CMC value. The nonionic surfactant has no charge repulsion interaction between head group which leads to lower the CMC value. While, anionic extended surfactants with higher PO groups in their alkyl chain has lower CMC owing to PO groups expand their hydrophobicity of the surfactant tail.

Addition of salts (electrolytes) affect on the CMC of anionic surfactant. It can be seen from Figure 4.3 that the anionic surfactant systems without salt addition has more CMC value than that of added salt system. The effect of added salt causes decreased in electrical repulsion between head groups and thus led to tighter packing of hydrophilic groups (Tongcumpou *et al.*, 2003). This is comparable with previous observations that anionic extended surfactant without salt addition had higher CMC value than those of system with adding 0.2M NaCl (Witthayapanyanon *et al.*, 2006). Thus, electrolytes in anionic surfactant solution correspond to reduce repulsion force of head group resulting in CMC reduction.

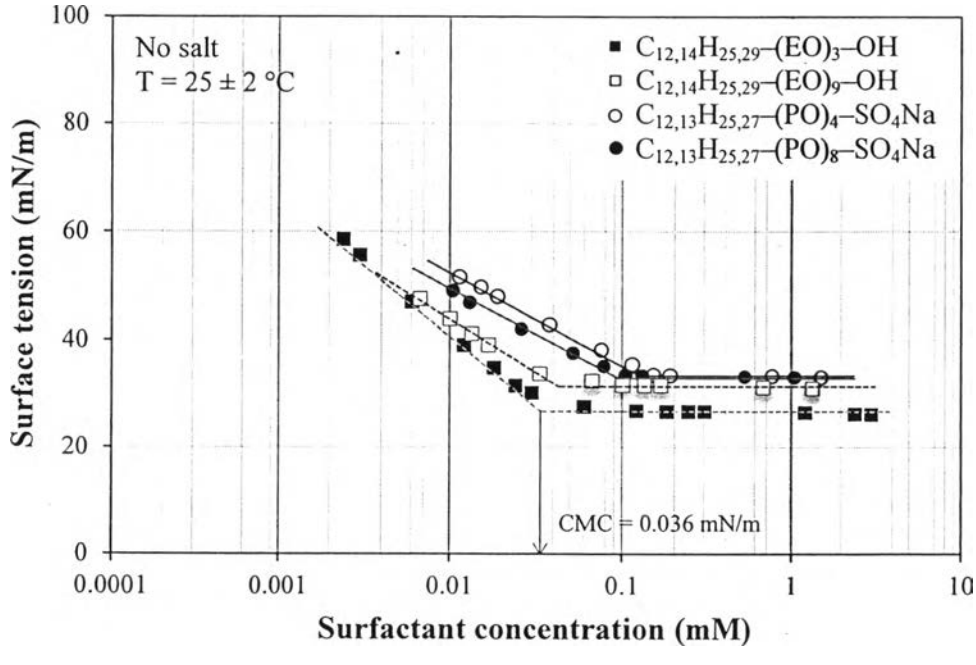

Figure 4.2 Critical micelle concentration of anionic extended and nonionic surfactant.

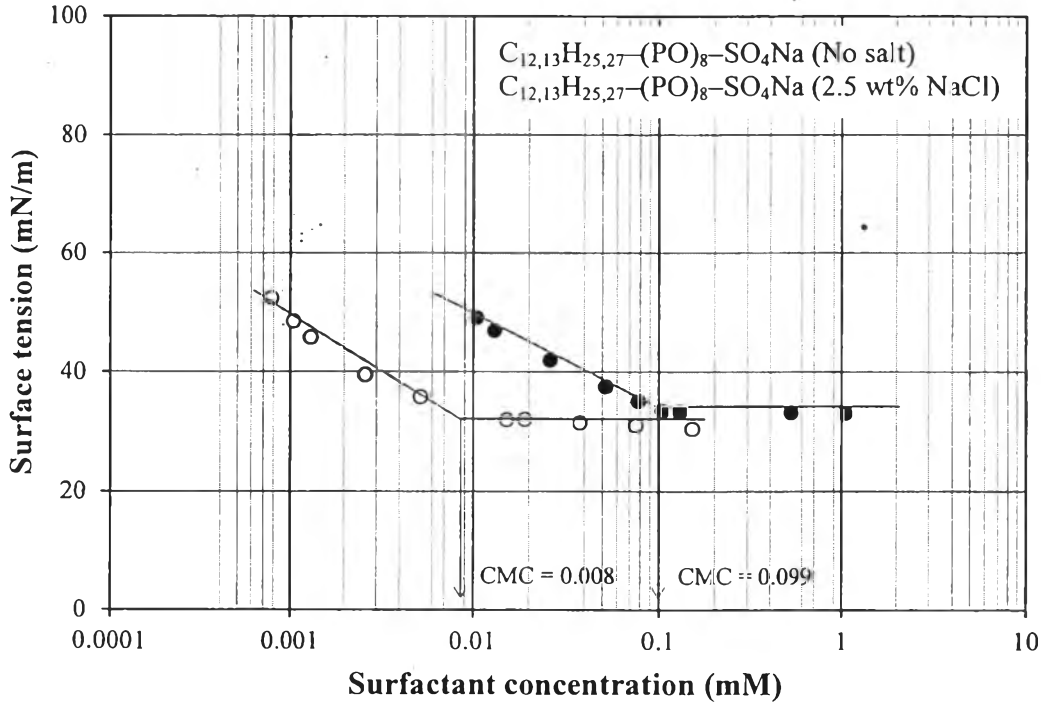

Figure 4.3 Critical micelle concentration of $C_{12,13}H_{25,27}$–$(PO)_8$–SO_4Na with and without salt at 25 ± 2 °C.

4.1.1.3 Adsorption at Liquid and Air Interface

The addition of surfactant in solution results in micelle formation, the surfactant monomers are considered to be in thermodynamic equilibrium with the micelles and with the adsorbed molecules at the air-liquid interface. The equilibrium concept of surfactant self-aggregation and adsorption is depicted in Figure 4.4. Thus, this surfactant concentration and the size of surfactant at interface region are presented by surface excess concentration (Γ) and area per molecule (A_{min}). These parameters are determined from the slope of the plot between surface tension versus surfactant concentration (log) and substituted in Gibbs adsorption equation (Mukherjee *et al.*, 2013). For instance, the slope of $C_{12,14}H_{25,29}$–$(EO)_3$–OH was obtained from Figure 4.5. According to the adsorption of two surfactant types at liquid and air interface (Table 4.1). It is found that the nonionic surfactant had a higher adsorption capacity (Γ) than the anionic extended surfactants. The nonionic surfactant, $C_{12,14}H_{25,29}$–$(EO)_3$–OH, had minimum area of surfactant aggregation leading to be the highest amount surfactant adsorbed on the interface. On

the other hand, the smallest amount of anionic extended surfactant, $C_{12,13}H_{25,27}$–$(PO)_8$–SO_4Na, adsorbed was required for surface coverage at the interface because of the repulsion between anionic head group and the coiling effect of PO groups. It is obvious to note that not only the effect of size and charge of the head group but also the effect of PO and EO groups caused plenty packing of surfactant aggregated at the interface region (Arpornpong *et al.*, 2010).

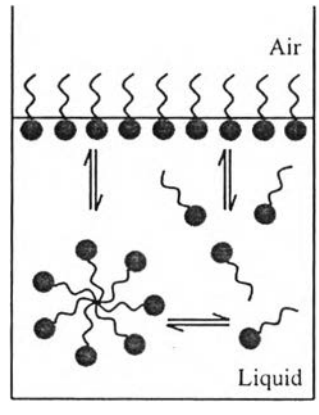

Figure 4.4 Schematic representation of micelle equilibriums.

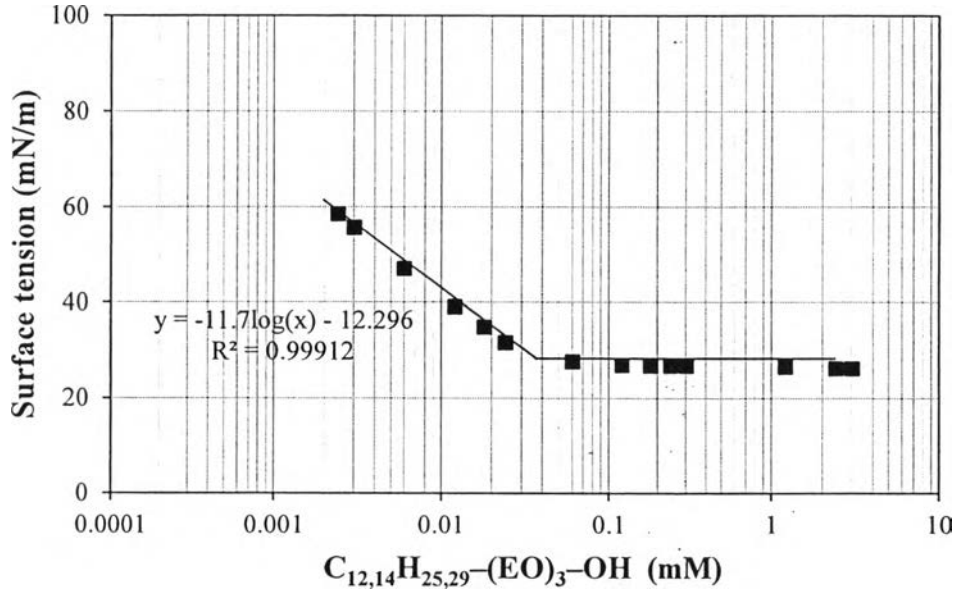

Figure 4.5 Relation between surface tension and $C_{12,14}H_{25,29}$–$(EO)_3$–OH concentration (log).

4.1.2 Microemulsion Phase Behavior

The microemulsion types (Winsor type I, II and III) are identified by visual observation as a classical method. Microemulsion phases were performed by adding an equal volume of an aqueous and crude palm oil phases and then left at incubator (30 ± 2 °C) to reach equilibrium. In addition, the samples were then placed for two weeks to ensure the phase transition of the microemulsion. A microemulsion solution contained different concentrations of surfactant and salt.

4.1.2.1 Salinity Scan

Microemulsion systems, in which anionic surfactants are presented, commonly use an electrolyte concentration as a scan variable to observe phase transformation and estimate an optimum salinity (Winsor type III). Phase transitions with varying salinities were prepared at the surfactant concentration of 0.5 wt%, as shown in Figure 4.6 and 4.7. The $C_{12,13}H_{25,27}$–$(PO)_4$–SO_4Na system was observed by emulsion phase (slightly turbid) placed in the center between two liquid phases at range of 0-1 wt% NaCl. When surfactant concentration reached to 3 wt%, small oil droplets stuck on the tube wall in turbid aqueous solution. At high salt concentration, the higher number of oil droplets as well as the more clearly aqueous solution was observed. Due to the fact that the $C_{12,13}H_{25,27}$–$(PO)_4$–SO_4Na has not enough potential interaction with crude palm oil for oil solubilization into upper phase. The phase transition of $C_{12,13}H_{25,27}$–$(PO)_8$–SO_4Na system was not significantly different from that in $C_{12,13}H_{25,27}$–$(PO)_4$–SO_4Na system. A packed emulsion phase in anionic surfactant system with eight PO groups appeared at the center between two liquid phases. A lower amount of oil droplets were observed comparing with previous system. It is noticeable that the extended surfactants with higher PO groups were more effective interaction with crude palm oil as well as oil solubilization than that of the lower number of PO groups system.

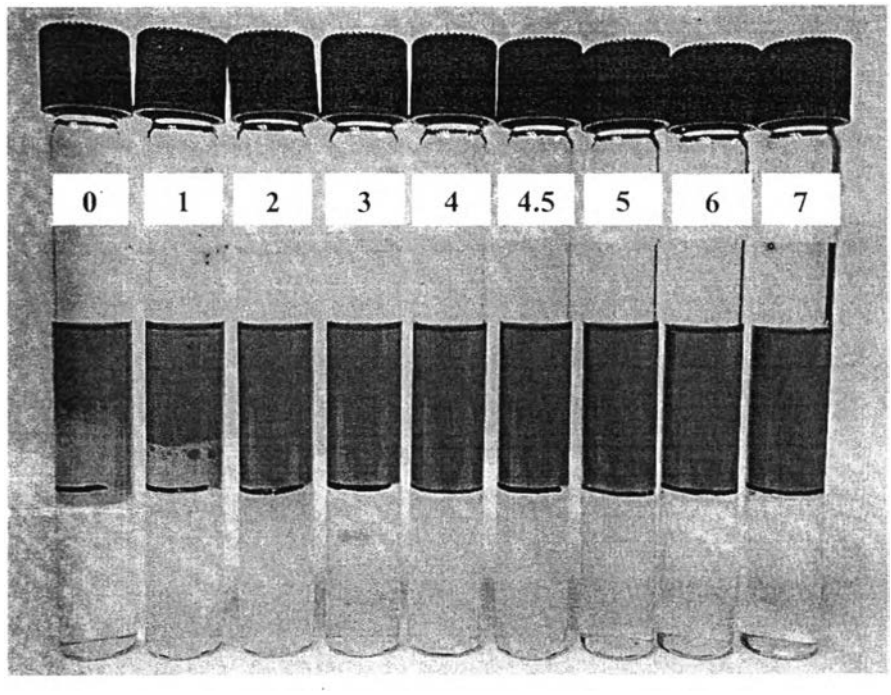

Figure 4.6 Microemulsion phase behavior of $C_{12,13}H_{25,27}$–$(PO)_4$–SO_4Na systems as a function of salt concentration (wt%) at 30 ± 2 °C.

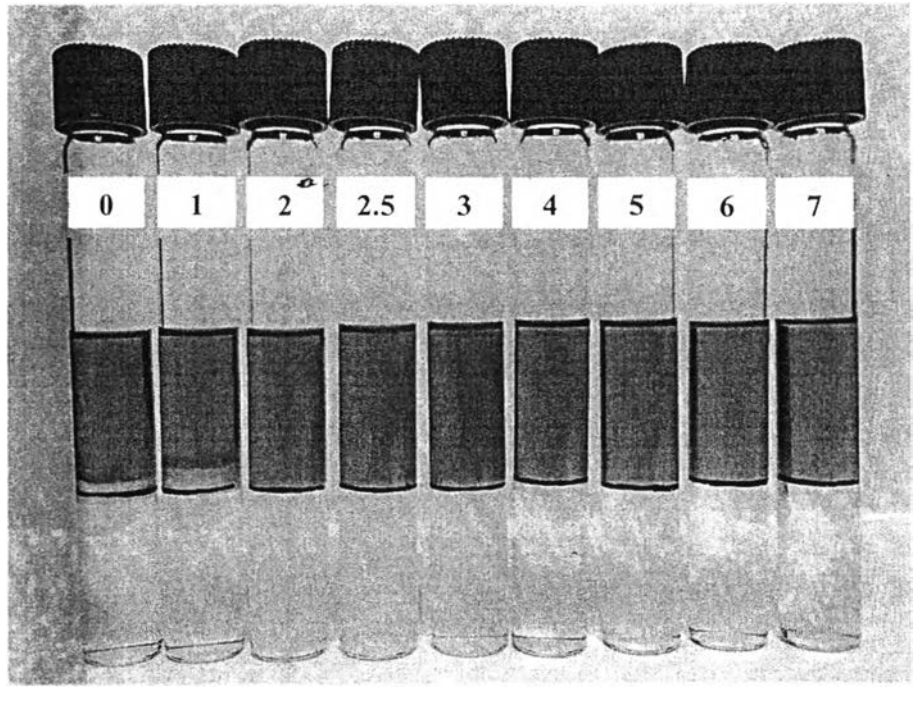

Figure 4.7 Microemulsion phase behavior of $C_{12,13}H_{25,27}$–$(PO)_8$–SO_4Na systems as a function of salt concentration (wt%) at 30 ± 2 °C.

In addition, a laser light beam is one technique to confirm microemulsions. When a laser light beam passes through a surfactant solution containing micelles, the cross polarizer is observed because the laser light beam is supposed to be diffused by a micelle or microemulsion phase and does not observed in pure water or oil phase (Thakur *et al.*, 2007). Note that, light beam could pass through the oil phase (crude palm oil) as illustrated in Figure 4.8. It is reasonable that crude palm oil composes of amphiphile molecule or natural surfactant e.g., free fatty acids and phospholipid. Free fatty acid (6.75%) which commonly contains in crude palm oil, is a carboxylic acid with a long hydrocarbon chain and phospholipid of 0.8-3.3 ppm (Goh *et al.*, 1984) consist of hydrophilic head with negatively charged phosphate group and glycerol and two hydrophobic tails of fatty acid hydrocarbon chains. The structure of these molecules can form aggregates as micelles.

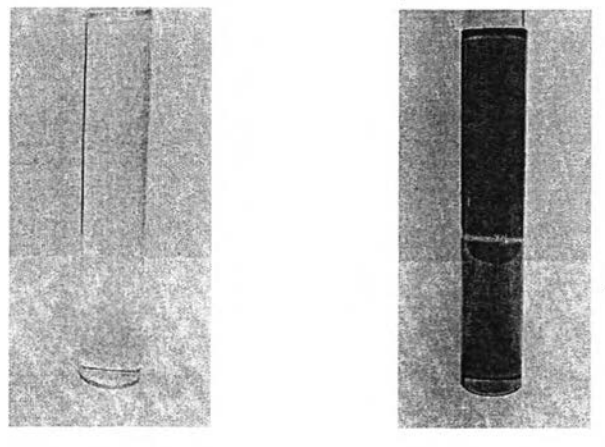

Figure 4.8 Laser light through (a) distillated water (b) crude palm oil.

4.1.2.2 Surfactant Concentration Scan

The Winsor type III region (see Figure 4.9) where have three phases; upper phase, middle phase and lower phase presented in the system was required for extracting oil application. Thus, all surfactant systems with either fixed salt concentration or temperature (anionic extended and nonionic surfactant, respectively) were varied by surfactant concentration.

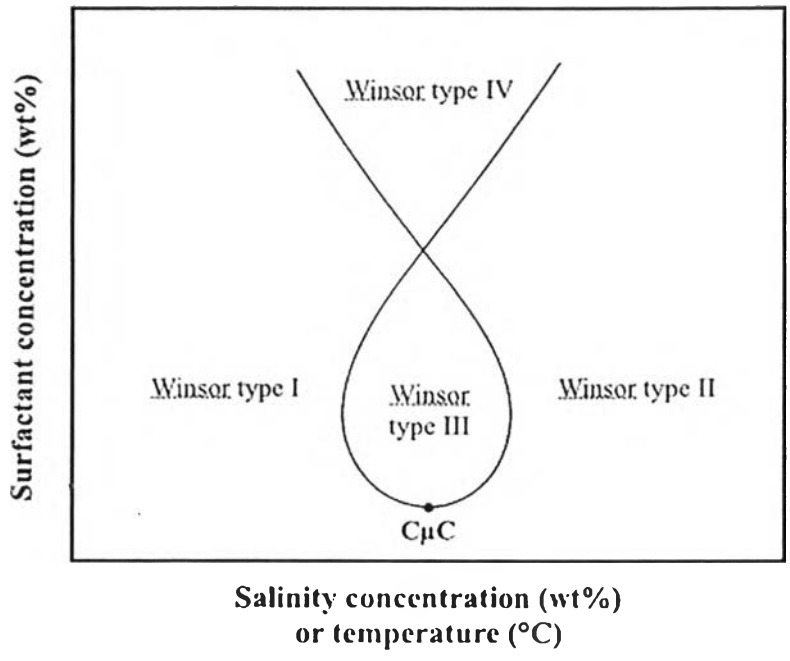

Figure 4.9 Fish diagram.

To begin with anionic extended surfactant, phase transition with varied surfactant concentration were prepared at salt concentration of 5 and 2.5 wt% (optimum salinity) for $C_{12,13}H_{25,27}$–$(PO)_4$–SO_4Na and $C_{12,13}H_{25,27}$–$(PO)_8$–SO_4Na systems, respectively. At the lowest surfactant concentration, the oil droplets dispersed on the tube wall as presented in Figure 4.10 and 4.11. From the results, the lower liquid phase of $C_{12,13}H_{25,27}$–$(PO)_4$–SO_4Na systems had clearly different compared to those of $C_{12,13}H_{25,27}$–$(PO)_8$–SO_4Na systems. The yellow transparent phase presented between two aqueous phase at 0.3 wt% $C_{12,13}H_{25,27}$–$(PO)_4$–SO_4Na and slowly extended with increasing surfactant concentrations. For analysis by laser light beam analysis, the very thin transparent phase of $C_{12,13}H_{25,27}$–$(PO)_4$–SO_4Na at the range of 0.3-0.8 wt% was reflected with the light beam (see Figure 4.12). At the same time, the reflection of light occurred at 0.2 wt% of $C_{12,13}H_{25,27}$–$(PO)_8$–SO_4Na. It is obvious to note that this region consists of micelles. However, both of phase scans were difficult to confirm the middle phase microemulsion formation.

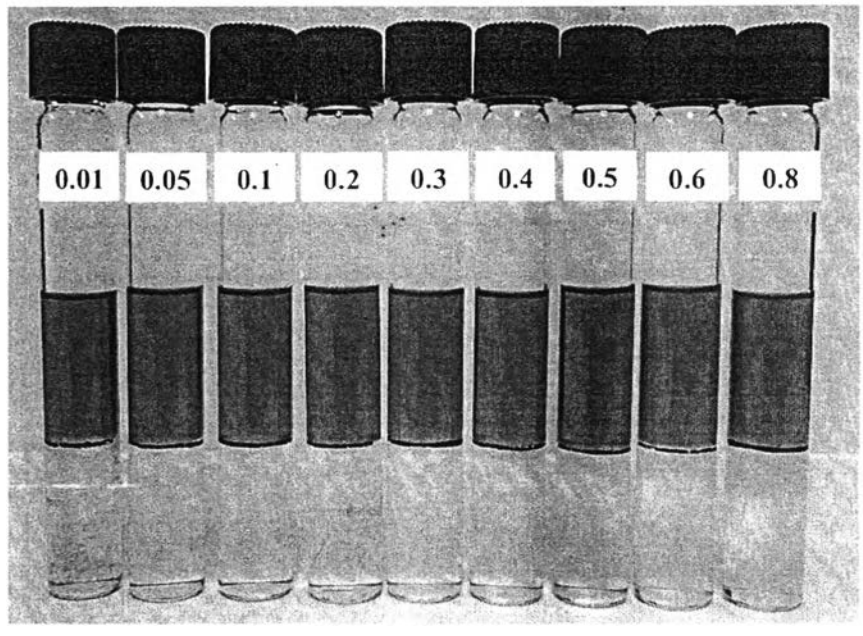

Figure 4.10 Microemulsion phase behavior of $C_{12,13}H_{25,27}$–$(PO)_4$–SO_4Na systems as a function of surfactant concentration (wt%) at 30 ± 2 °C.

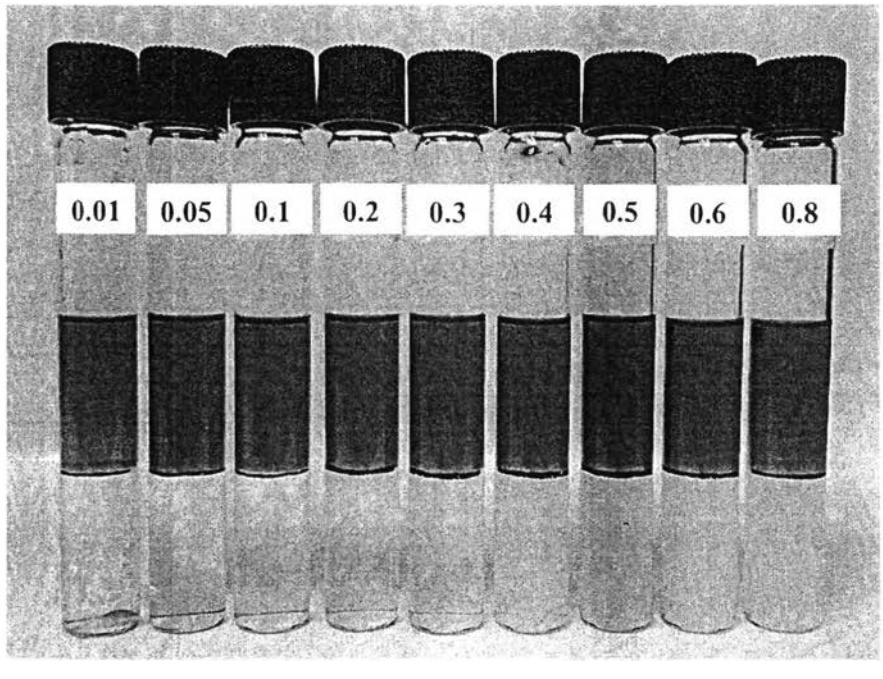

Figure 4.11 Microemulsion phase behavior of $C_{12,13}H_{25,27}$–$(PO)_8$–SO_4Na systems as a function of surfactant concentration (wt%) at 30 ± 2 °C.

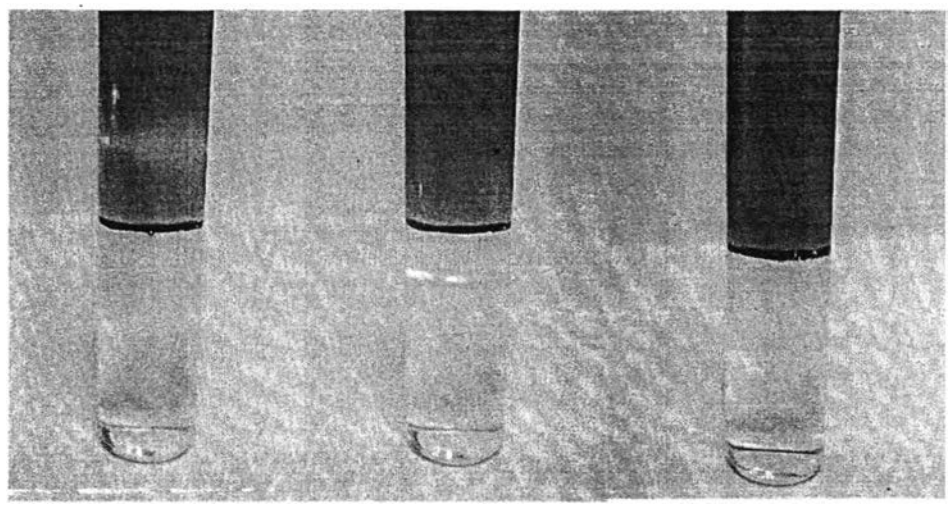

(a) (b) (c)

Figure 4.12 Laser light beam through (a) oil phase (b) yellow transparent phase (c) bottom phase at 0.8 wt% of $C_{12,13}H_{25,27}$–$(PO)_4$–SO_4Na system.

Moving to nonionic surfactant, phase transition of nonionic surfactant normally requires temperature to change phase. This work, the experimental set up for suitable extraction method was designed to operate at room temperature condition. Figure 4.13 and 4.14 present microemulsion phase behaviors of surfactant systems with different EO group, namely $C_{12,14}H_{25,29}$–$(EO)_3$–OH and $C_{12,14}H_{25,29}$–$(EO)_9$–OH, respectively. For $C_{12,14}H_{25,29}$–$(EO)_3$–OH system, oil droplets appeared at low surfactant concentration and then theirs size gradually reduced until reaching surfactant concentration of 4 wt%. At near middle between two phases, there was an emulsion phase. Additionally, appearance of bottom phase was more turbid at the end of phase scan. In the case of $C_{12,14}H_{25,29}$–$(EO)_9$–OH system, small size of oil droplet was observed at the beginning of surfactant concentration after that the emulsion phase appears at 0.2 wt% and the height of this phase went up to equate the top of liquid phase with increasing surfactant concentration. For bottom liquid phase, it was yellow clear solution. The $C_{12,14}H_{25,29}$–$(EO)_3$–OH system was completely different from $C_{12,14}H_{25,29}$–$(EO)_9$–OH system due to the effect of EO group. In addition, a laser light beam could pass through not only the oil phase but also the aqueous phase of both nonionic systems.

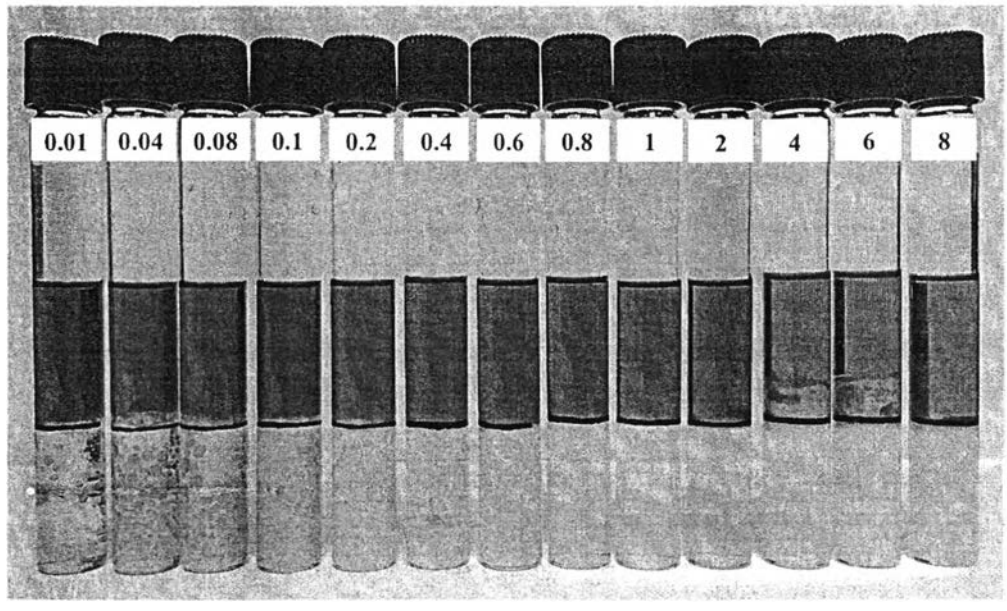

Figure 4.13 Microemulsion phase behavior of $C_{12,14}H_{25,29}$–$(EO)_3$–OH systems as a function of surfactant concentration (wt%) at 30 ± 2 °C.

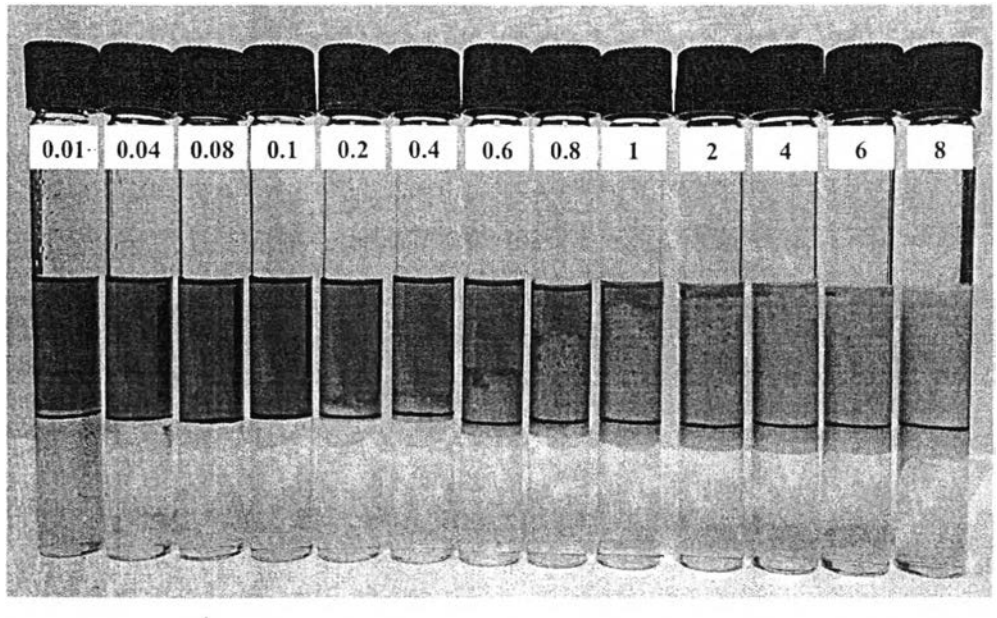

Figure 4.14 Microemulsion phase behavior of $C_{12,14}H_{25,29}$–$(EO)_9$–OH systems as a function of surfactant concentration (wt%) at 30 ± 2 °C.

In conclusion, the middle phase microemulsion of all surfactant systems were not clearly seen by visual observation and laser light technique. It could be due to the fact that crude palm oil contains complex ingredients such as a mixture of triglycerides, phospholipids, fatty acids, metals trace and oxidizing compounds, in accordance with the problem occurred in Thakur *et al.* (2007). Thus, an alternative method to determine the optimum salinity and formulation was studied. The interfacial tension (IFT) measurement has been proven in the middle phase at which the lowest IFT were presented. As an illustration, the systems of various anionic extended surfactants and oils were determined optimum salinity and critical microemulsion concentration (CμC) point by measuring IFT (Witthayapanyanon *et al.*, 2006). For Do and Sabatini (2010) study, the ultralow IFT as optimum formulation of anionic extended surfactants was measured for vegetable oil extraction. Thus, the IFT measurement would be used to investigate the optimum salinity of the microemulsion formulation.

4.1.3 Interfacial Tension Measurement

The change of microemulsion phase behavior is described by Winsor type. Thus, IFT is an effective parameter to indicated microemulsion transition and optimum formulation. The IFT measurements are conducted as a function of salt and surfactant concentration in order to estimate the point at which IFT between middle phase of the excess oil or excess water phase become an equal and attains the lowest IFT.

4.1.3.1 Effect of Salt Concentration

Salinity scans of anionic surfactant in this study are shown in Figure 4.15. Both $C_{12,13}$-$(PO)_4$-SO_4Na and $C_{12,13}$-$(PO)_8$-SO_4Na systems were prepared at 0.5 wt% to determine the optimum salinity (S*) of each system. The optimum salinity indicates the appropriate electrolyte concentration of the surfactant system at which attains minimum IFT. The results show that anionic extended surfactant systems were able to produce an ultralow IFT (<0.1 mN/m) with crude palm oil. The lowest IFT of $C_{12,13}$-$(PO)_4$-SO_4Na was 0.015 mN/m with S* of 5 wt% NaCl and $C_{12,13}$-$(PO)_8$-SO_4Na was 0.005 mN/m with S* of 2.5 wt% NaCl. It is noticed that the number of PO groups increased, the optimum salinity and minimum

IFT decreased due to the fact that the PO groups increase hydrophobicity of the surfactant tail. It is a good agreement in the ultralow IFT value between anionic extended surfactant and various vegetable oils (palm oil) studied by Phan *et al.* (2010). The ultralow IFT (0.0057 mN/m) of $C_{14,15}$-$(PO)_8$-SO_4Na with palm oil was reported by Witthayapanyanon *et al.* (2006). Concisely, these anionic extended surfactants using low salt concentration could produce an ultralow IFT with crude palm oil and without addition of co-oils and/or alcohol. The anionic surfactant having high hydrophobic part (PO groups) impacted on the IFT reduction.

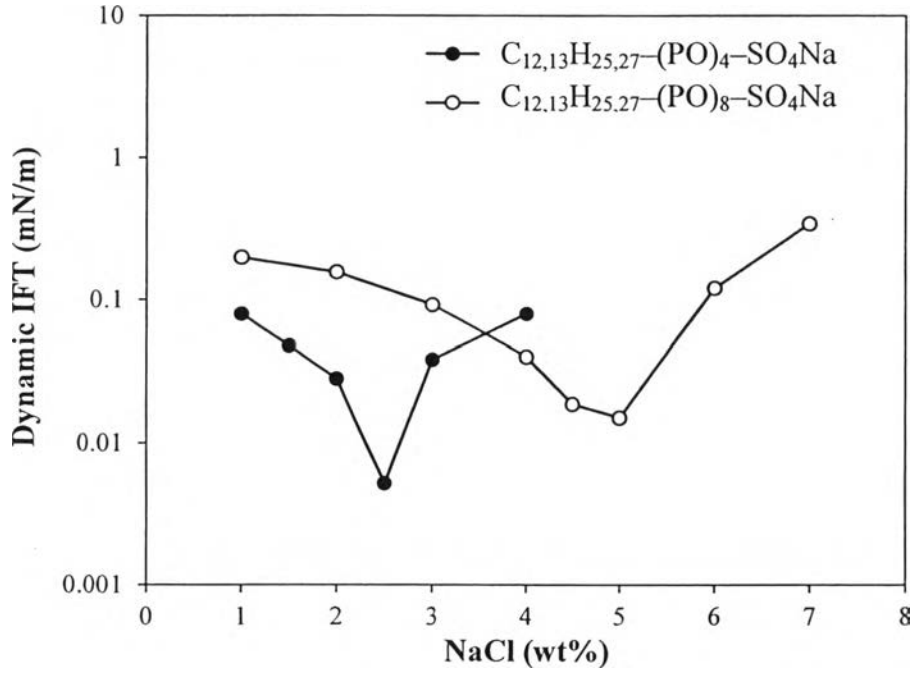

Figure 4.15 Dynamic IFT versus salt concentration at anionic extended surfactant concentration of 0.5 wt% at 25 ± 2 °C.

4.1.3.2 Effect of Surfactant Concentration

In this set study, the IFT between surfactant solution and crude palm oil was measured by varying surfactant concentrations with fixed optimum salinity. Figure 4.16 shows the dynamic IFT for $C_{12,13}$-$(PO)_4$-SO_4Na and $C_{12,13}$-$(PO)_8$-SO_4Na with 5 and 2.5 wt%, respectively. It can be seen that the decrease in two stages was observed for both surfactant systems as similar trends in preceding

literature (Witthayapanyanon *et al.*, 2006). The first stage corresponds to aggregation of surfactant monomers to form micelle which refers to critical micelle concentration (CMC). The second stage corresponds to change in curvature of the micelle until at the end of point where the first droplet of microemulsions is formed. This concentration is known as critical microemulsions concentration (CμC). The CμC values of $C_{12,13}$-$(PO)_4$-SO_4Na (0.4 wt%) had nearly twice to the CμC of $C_{12,13}$-$(PO)_8$-SO_4Na (0.2 wt%). The lower CMC of anionic extended surfactant systems was consistent with the lower CμC observed for this surfactant. Moreover, the $C_{12,13}$-$(PO)_8$-SO_4Na system using lower surfactant concentration could reduce a larger IFT value with crude palm oil compared to that of $C_{12,13}$-$(PO)_4$-SO_4Na system. Thus, the introduction of PO groups had a significant effect on microemulsion formation with crude palm oil.

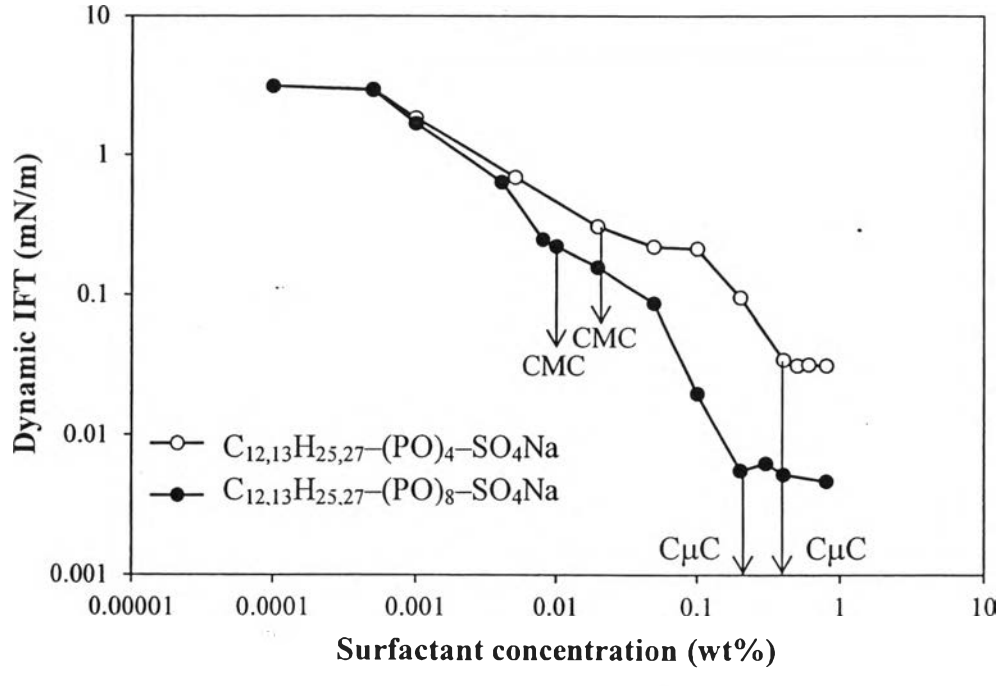

Figure 4.16 Dynamic IFT versus surfactant concentration at optimum salinity of 5 and 2.5 wt% for $C_{12,13}H_{25,27}$–$(PO)_4$–SO_4Na and $C_{12,13}H_{25,27}$–$(PO)_8$–SO_4Na systems, respectively at 25 ± 2 °C.

In Figure 4.17, the CμC points of nonionic surfactant are not observed because these surfactants depend on temperature to form phase transition. This research focused the operating condition of room temperature led to residual oil extraction at room temperature. According to Figure 4.9, temperature is a significant parameter of the middle phase formation for nonionic surfactant. Hence, the oil extraction at room temperature was not suitable to formulate middle phase with crude palm oil for both nonionic surfactant. Although $C_{12,14}H_{25,29}$–$(EO)_9$–OH system provided lower IFT value than that of $C_{12,14}H_{25,29}$–$(EO)_3$–OH system (the lowest IFT of nonionic surfactants with three and nine EO groups were 0.853 and 0.224 mN/m, respectively), they did not achieve an ultralow IFT (<0.1 mN/m as reported in Phan *et al.* (2011)). In other words, the efficiency of these nonionic surfactant systems were insufficient for reducing the IFT with crude palm oil at 25 ± 2 °C.

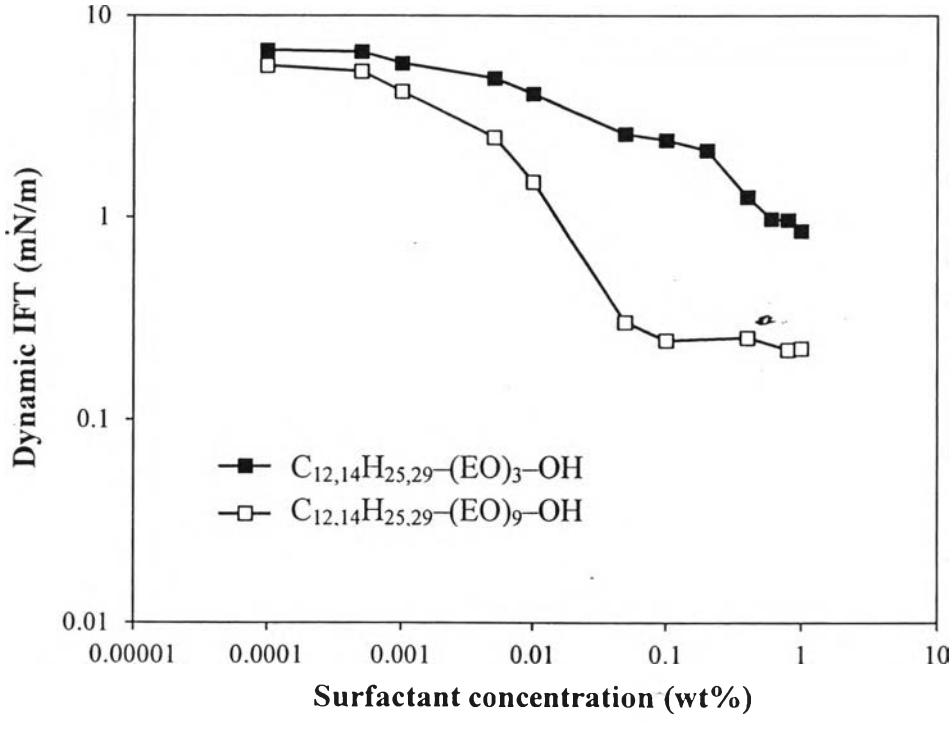

Figure 4.17 Dynamic IFT versus surfactant concentration of $C_{12,14}H_{25,29}$–$(EO)_3$–OH and $C_{12,14}H_{25,29}$–$(EO)_9$–OH systems at 25 ± 2 °C.

From Figure 4.18 presents comparisons of anionic extended surfactants ($C_{12,13}H_{25,27}$–$(PO)_4$–SO_4Na and $C_{12,13}H_{25,27}$–$(PO)_8$–SO_4Na) and nonionic surfactants ($C_{12,14}H_{25,29}$–$(EO)_3$–OH and $C_{12,14}H_{25,29}$–$(EO)_9$–OH). The result shows that anionic head group (sulfate) with PO groups produced lower IFT than that of nonionic head group (alcohol) with EO groups as the extended part. It is encouraging to note that sulfate and PO group has a potential interaction with crude palm oil, which contains triglycerides as a main component (triglyceride is glycerol group with three hydrocarbon chains or high hydrophobic oils with a polar nature). Additionally, anionic extended surfactant could achieve the minimum IFT with crude palm oil at 25 ± 2 °C. Therefore, these surfactant systems could produce the lowest IFT as well as highest oil extraction efficiency for oil extraction process. The result of Kadioglu *et al.* (2011) is a good support to this observation.

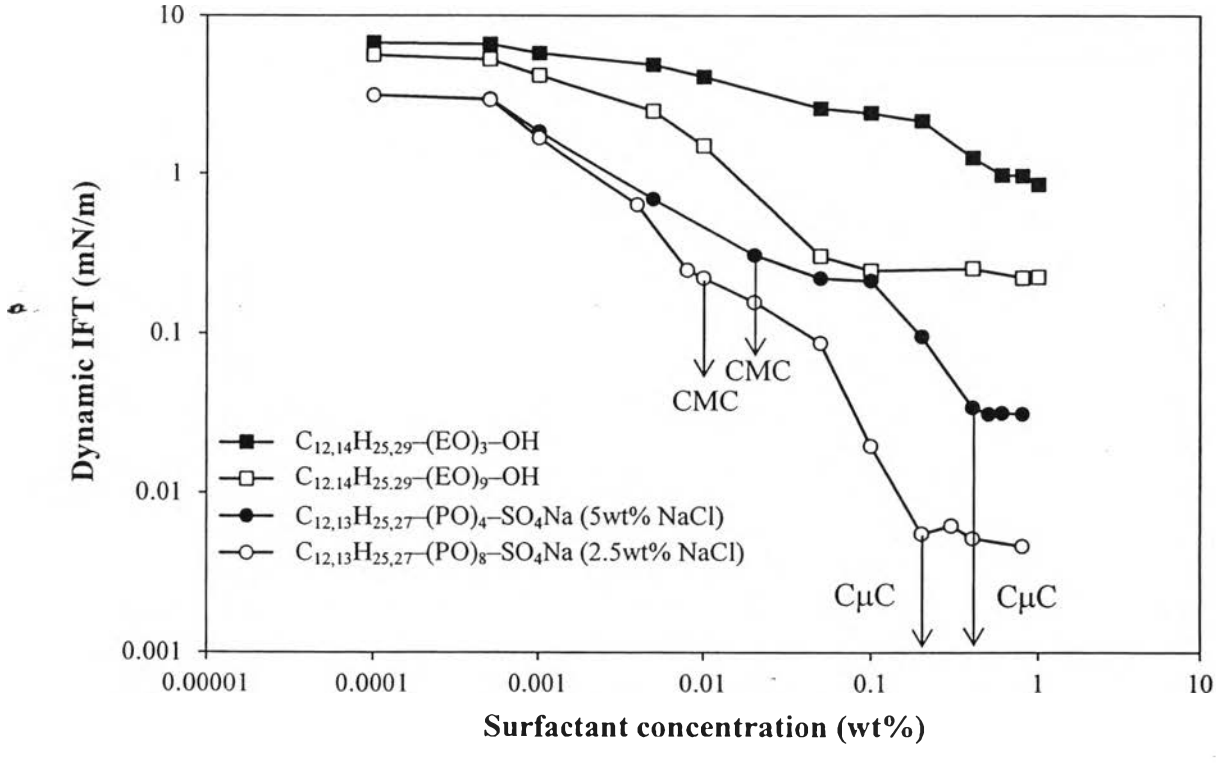

Figure 4.18 Dynamic IFT versus anionic extended and nonionic surfactant concentration at 25 ± 2 °C.

Table 4.2 CMC, area per molecule and minimum IFT at optimum salt for anionic surfactant and without salt for nonionic surfactant

Surfactant	CMC in mM (wt%) at water-oil	A_{min} ($Å^2$)	Minimum IFT (mN/m)
$C_{12,14}H_{25,29}$–$(EO)_3$–OH	0.036 (1.2×10^{-3})	81	0.853
$C_{12,14}H_{25,29}$–$(EO)_9$–OH	0.045 (2.7×10^{-3})	116	0.224
$C_{12,13}H_{25,27}$–$(PO)_4$–SO_4Na	0.012 (6.3×10^{-4})	104	0.031
$C_{12,13}H_{25,27}$–$(PO)_8$–SO_4Na	0.008 (6.1×10^{-4})	110	0.005

In addition, the measurement of CMC (Table 4.2) and A_{min} were evaluated at the optimum salt for anionic extended surfactant and compared to those of nonionic surfactant without adding salt. The result indicated a dropped in CMC of anionic extended surfactant systems as the alkyl chain length increased, resulting in 0.012 and 0.008 mM for $C_{12,13}H_{25,27}$–$(PO)_4$–SO_4Na and $C_{12,13}H_{25,27}$–$(PO)_8$–SO_4Na, respectively. To compare CMCs value of anionic extended surfactant from the results in Table 4.2 (water-air interface) and Figure 4.16 (water-oil interface), the CMC value of water and oil was not the same as that of water and air interface. However, the $C_{12,13}H_{25,27}$–$(PO)_8$–SO_4Na system had the lowest CMC value at water-air interface. For area per molecule of all surfactant systems, it is obvious to note that anionic extended surfactants have large area per molecule, but they still produce lower CMC values and ultralow IFT. Witthayapanyanon *et al.* (2006) suggested that the adding of PO groups resulted in an increase the hydrophobic interaction that helps offset the lower packing density.

For all the reasons mentioned above, the presence of either EO or PO groups inserted between head and tail part has a significant effect on the CMC and area per molecule of the surfactant system. It can be concluded that the surfactant having higher PO group with sulfated head group has a unique characteristic for microemulsion formation with crude palm oil. The presence of PO groups supports an increase in hydrophobicity and extended hydrocarbon chain and a sulfated head

group conducts to a strong interaction with high hydrophobic oil which results an ultralow IFT with crude palm oil. For nonionic surfactant, IFT between surfactant and crude palm oil could not achieve an ultralow IFT owing to the limited temperature and their structure in microemulsion phase formulation. Thus, the property of surfactant used for microemulsion formulation in this study would be an anionic surfactant with PO groups.

4.2 Oil Extraction

In previous section, the crucial property of appropriate surfactant system for oil extraction which is able to achieve ultralow IFT with crude palm oil at room temperature without adding co-surfactant. However, another important role for oil extraction is a contact time because the interaction between oil and surfactant requires adequately period of time to reach its equilibrium for oil detachment from SBE's surface. All surfactants at the lowest IFT are presented in Figure 4.19. It is observed that the IFT values of all surfactant systems decreased dramatically in first 5 min and then kept constant until 20 min. It can be referred that the equilibrium time of crude palm oil and surfactant solution is within 20 min. Hence, this optimum time was used as an initial contact time in oil extraction process.

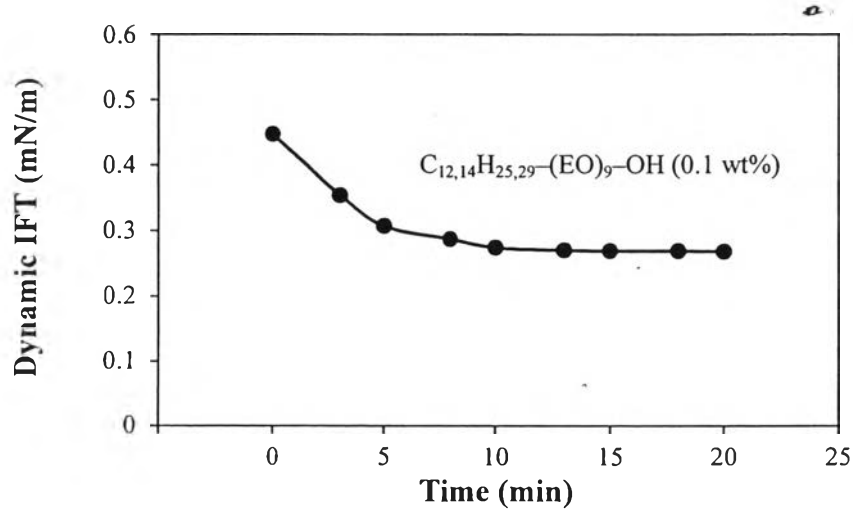

Figure 4.19 Dynamic IFT as a function of time of $C_{12,14}$-$(EO)_9$-OH system with crude palm oil at 25 ± 2 °C.

The procedure for oil extraction by surfactant was carried out using 30 ml surfactant solution, 1000 rpm, 20 min of contact time and 3 g SBE loading at room temperature. The three fractions are obtained; free oil refers to the amount of oil on the top phase, oil in emulsion solution, and residual oil which refers to oil remaining in SBE after three times of washing residual SBE. Weight of free oil based on total oil content in SBE (hexane extraction) was defined as free oil extraction efficiency. Total oil extraction efficiency referred to difference between weight of total oil content and residual oil in SBE based on total oil content. It is significant to note that this extraction process commonly used for analytical quantification only which was presented in many literatures for vegetable oil extraction using surfactant extraction. (Do and Sabatini, 2010), (Kadioglu *et al.*, 2011) and (Tuntiwiwattanapun *et al.*, 2013)

Because of various samples for determining residual oil weight, the procedure of hexane extraction was conducted similar to surfactant technique instead of using soxhlet extraction. SBE was stirred 1000 rpm with 30 ml hexane for 20 min at room temperature. The hexane solution was removed with pipette, then evaporated at 110 °C and the extracted oil was then weighed. For oil extraction experiments, each sample was conducted in triplicate. In addition, total oil content in SBE was extracted by hexane as a residual oil extraction method. It should be to note that hexane extraction based on assumption of 100% oil yield was calculated as the total oil content in SBE of 21.02 wt%.

In oil extraction, the important parameters based on extraction efficiency were selected including the effects of surfactant type, salt concentration, surfactant concentration, extraction time and SBE loading.

4.2.1 Effect of Surfactant Structure

Anionic extended surfactant systems were prepared at 1 wt% at the optimum salt concentration. As seen in Figure 4.20, the $C_{12,13}H_{25,27}$–$(PO)_4$–SO_4Na system composed of emulsion phase which is undesirable in extraction application. In contrast, $C_{12,13}H_{25,27}$–$(PO)_8$–SO_4Na system produces free oil and emulsion phase. It is observed that majority of extracted oils solubilized in the emulsion phase whereas minority of those oils existed in free oil phase. The amount of oil extracted

using $C_{12,13}H_{25,27}$–$(PO)_4$–SO_4Na was lower than the recovered oil obtained $C_{12,13}H_{25,27}$–$(PO)_8$–SO_4Na. The area per molecule data from Table 4.2 was also supported the surfactant adsorption on oil-water interface. It can be clearly seen that the molecule of anionic extended surfactant with eight PO groups had larger area per molecule (extended hydrocarbon chain) resulting in greater IFT reduction compared to that with four PO groups. This result is agreed with study of Do and Sabatini (2010). The anionic extended surfactant provided lower IFT with peanut oil and canola oil would produce higher fraction of extracted oil. Hence, total oil extraction efficiency of $C_{12,13}H_{25,27}$–$(PO)_8$–SO_4Na was higher than that of $C_{12,13}H_{25,27}$–$(PO)_4$–SO_4Na.

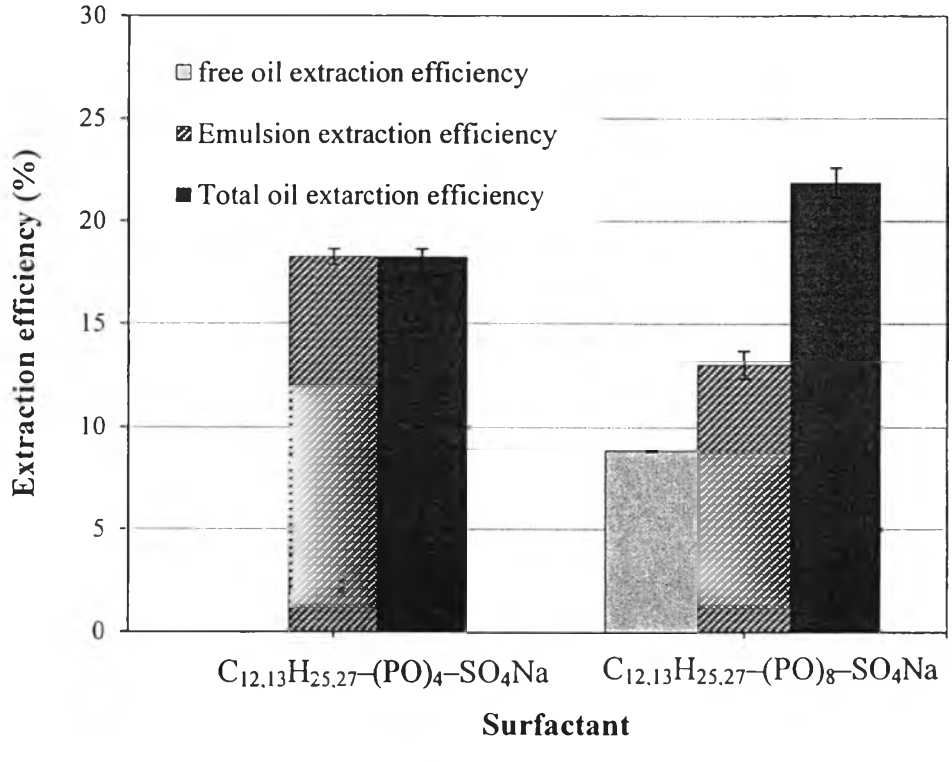

Figure 4.20 Extraction efficiency versus 1 wt% $C_{12,13}H_{25,27}$–$(PO)_4$–SO_4Na (5 wt%) and 1 wt% $C_{12,13}H_{25,27}$–$(PO)_8$–SO_4Na (2.5wt%) with 1000 rpm for 20 min using solid to liquid ratio 1/10.

For nonionic surfactant systems, the comparison of extraction efficiency between $C_{12,14}H_{25,29}$–$(EO)_3$–OH and $C_{12,14}H_{25,29}$–$(EO)_9$–OH systems are shown in Figure 4.21. The $C_{12,14}H_{25,29}$–$(EO)_3$–OH system produced fraction of free oil and emulsion phase where the extracted oil in free oil had more than that of emulsion. However, $C_{12,14}H_{25,29}$–$(EO)_3$–OH had lower amount of extracted oil than that of $C_{12,14}H_{25,29}$–$(EO)_9$–OH. For $C_{12,14}H_{25,29}$–$(EO)_9$–OH system, the oil dispersed in only emulsion phase. It can be explained from the IFT value with crude palm oil and the losses by surfactant adsorption at interface (see Table 4.2). Although, the nonionic surfactant with three EO group had higher amount of molecule adsorbed on the oil surface, it was lower potential reduction of IFT (0.853 mN/m) resulting in very low total oil extraction. Thereby, the difference in the number of EO groups were a very significant effect on removal oil.

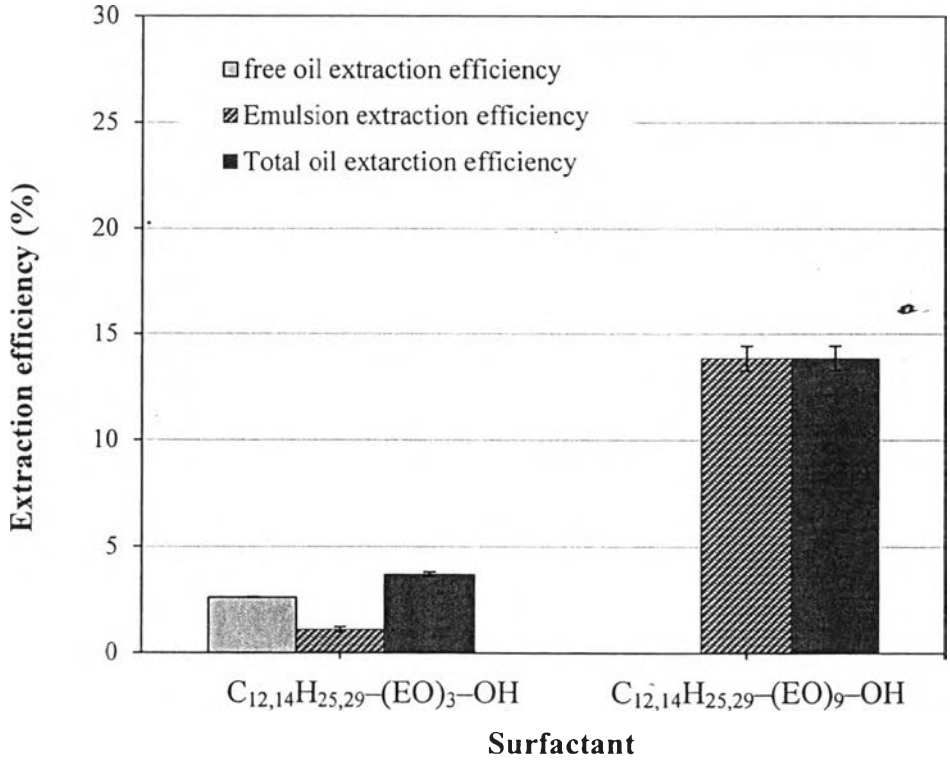

Figure 4.21 Extraction efficiency versus 1 wt% of and $C_{12,14}H_{25,29}$–$(EO)_9$–OH with 1000 rpm for 20 min using solid to liquid ratio 1/10.

Furthermore, the head group structure also affected on extraction efficiency. Comparison the result of minimum IFT (see Table 4.2) and total oil extraction efficiency presented in Figure 4.22, the both of surfactants with sulfated head group provided higher fraction of total oil than that of surfactant containing alcohol head group. Meanwhile, they could produce lower IFT between crude palm oil and surfactant solution. It is indicated that their unique structure well interacted with the oil as a result of high oil removal efficiency.

Concisely, the anionic surfactant was more suitable than nonionic surfactant. However, there was a slight difference between $C_{12,13}H_{25,27}$–$(PO)_4$–SO_4Na and $C_{12,13}H_{25,27}$–$(PO)_8$–SO_4Na system accounting for 18 and 22%, respectively. Thus, only $C_{12,13}H_{25,27}$–$(PO)_8$–SO_4Na system was produced a free oil phase that was desirable for study in other parameters.

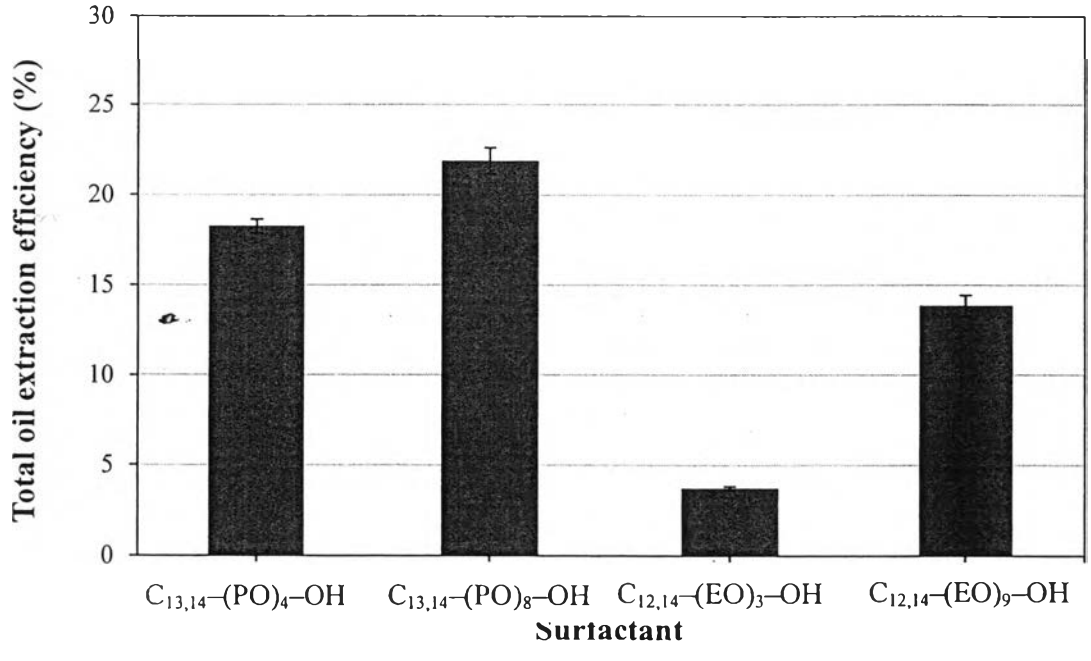

Figure 4.22 Total oil extraction efficiency versus 1 wt% of anionic extended and nonionic surfactant with 1000 rpm for 20 min using solid to liquid ratio 1/10.

4.2.2 Effect of Salt Concentration

As salt concentration affecting on micelle formation, the surfactant adsorption at liquid-air interface and IFT of microemulsion phase study (Section 4.1), the effect of salt also influenced oil extraction efficiency. The $C_{12,13}H_{25,27}$–$(PO)_8$–SO_4Na concentration of 0.5 wt% was varied in a range of 1-8 wt% NaCl. As seen from the Figure 4.23, the total oil extraction efficiency dramatically increased and then reached the highest value of about 20% at 2.5 wt% NaCl. As salt concentration increased further, there was a significant decrease in total oil extraction efficiency. Dynamic IFT results suggest that the IFT moderately decreased until the lowest IFT achieved at salt concentration of 2.5 wt%, it is an excellent agreement in maximum total oil extraction. After that upward trend of IFT was recorded as downward trend of fraction oil removal. This was consistent with previous study that observed the effect of salt concentration and dynamic IFT for peanut oil extraction (Do and Sabatini, 2010). Thus, the optimum salt concentration impacts the removal efficiency of oil from SBE. As it would help reduce the IFT between surfactant and crude palm oil, resulting in high fraction of detached oil. Furthermore, this optimum salinity is very low concentration with avoiding viscous solution. The $C_{12,13}H_{25,27}$–$(PO)_8$–SO_4Na at 2.5 wt% NaCl was used in next parameter study.

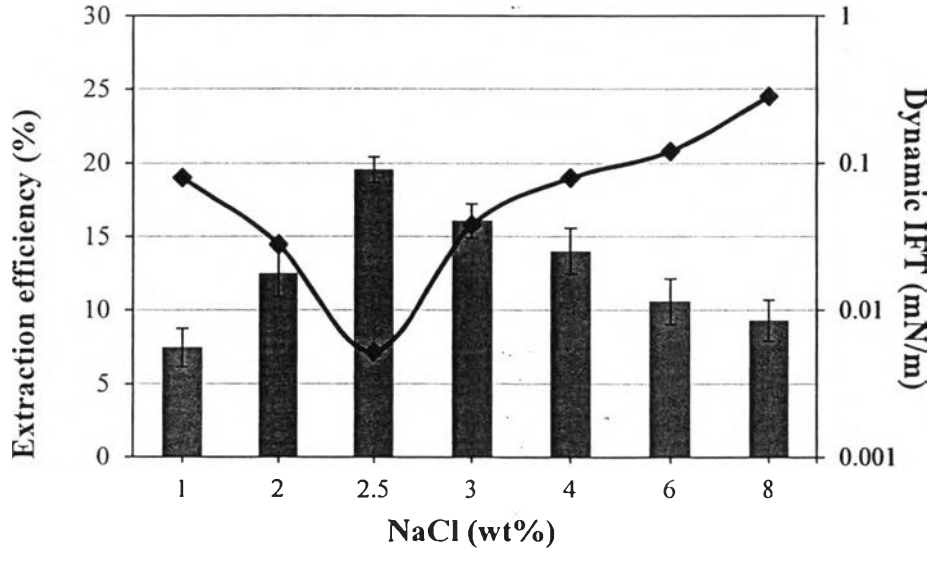

Figure 4.23 Extraction efficiency versus 0.5 wt% $C_{12,13}H_{25,27}$–$(PO)_8$–SO_4Na with 1000 rpm for 20 min using solid to liquid ratio 1/10.

4.2.3 Effect of Surfactant Concentration

From Figure 4.17 shows the relation of dynamic IFT and surfactant concentration and the CμC value of $C_{12,13}H_{25,27}$–$(PO)_8$–SO_4Na was 0.2 wt%. Therefore, the surfactant at optimum salt was varied above and below CμC value to study the effect of concentration on oil extraction efficiency. According to the Figure 4.24, the total oil extraction efficiency remained stable at below CμC value and increased continuously until its approached around 20% of extraction efficiency at surfactant concentration of 1 wt%. At the higher surfactant concentration, the total oil extraction efficiency did not change. The similar trend was observed in Do and Sabatini (2010). It is interesting to note that the higher amount of surfactant used for removing oil from SBE because of the losses from surfactant adsorption onto solid surface as the result observed from the solution after washing residual SBE. There was a cloudy solution due to dispersion of micelles. It can be concluded that the optimum surfactant used in oil extraction should be higher than the concentration at CμC value due to sufficient using of surfactant in oil adsolubilization and solubization instead of the surfactant losses on SBE surface. Hence, concentration of 1 w% $C_{12,13}H_{25,27}$–$(PO)_8$–SO_4Na at 2.5 wt% NaCl was used for study in next section.

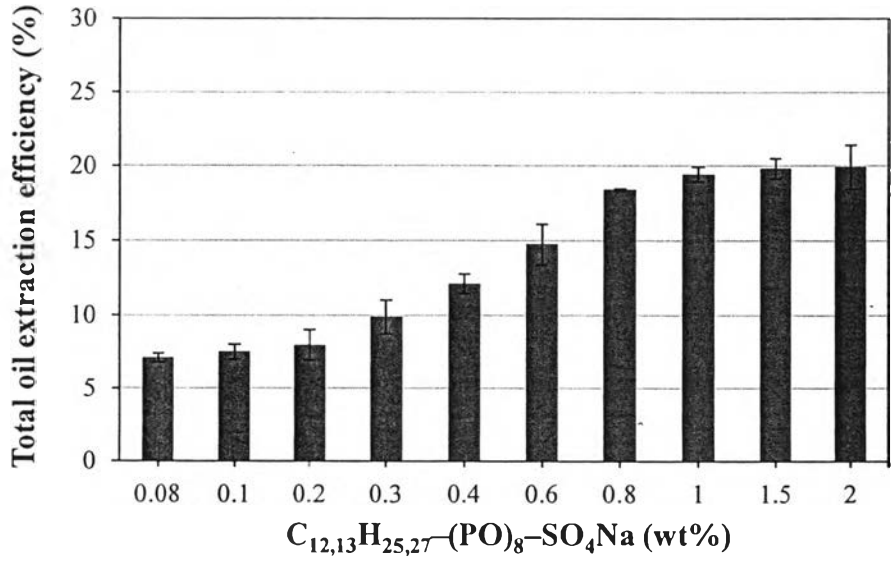

Figure 4.24 Total oil extraction efficiency versus 2.5 wt.% NaCl for $C_{12,13}H_{25,27}$–$(PO)_8$–SO_4Na system with 1000 rpm for 20 min using solid to liquid ratio 1/10.

4.2.4 Effect of Contact Time

The optimum contact time between surfactant and oil adsorbed on SBE is an important parameter that affects total oil extraction efficiency. In this experiment, the contact time was varied from 5, 10, 20, 30, 60 and 120 min according to total oil extraction efficiency. The results in Figure 4.25 shows that total oil extraction efficiency rises rapidly with increasing the contact time and then oil extraction efficiency is not change after 20 min. This is a good agreement with the trend of dynamic IFT, which presented that the IFT remains constant after 20 min. In other word, the IFT between surfactant solution and crude palm oil has reached equilibrium within 20 min. Thus, the optimum contact time for oil removal from SBE is then selected at 20 min. Although the highest total oil extraction efficiency was higher than 20%, it was much lower than that of relative extraction efficiency by hexane extraction (100%). Solid to liquid ration was required to study for improving oil extraction efficiency.

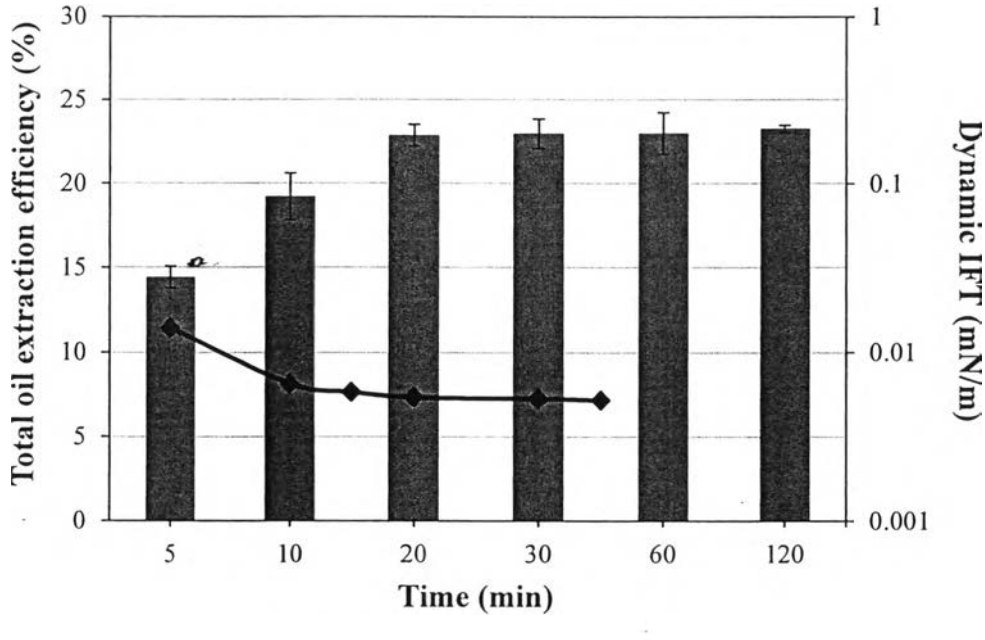

Figure 4.25 Total oil extraction efficiency versus 2.5 wt% NaCl for 1 wt% $C_{12,13}H_{25,27}$–$(PO)_8$–SO_4Na system with 1000 rpm for 20 min using solid to liquid ratio 1/10.

4.2.5 Effect of Soild to Liquid Ratio

Surfactant used in extraction study needs sufficient amount to adsorb on adsorbed oil as well as losses on SBE surface during extraction process. Thereby, weight of spent bleaching was properly loaded with desired volume of surfactant solution. From the SBE loading results shown in Figure 4.26, the SBE was prepared in different weight mixed with 30 ml of surfactant solution for 20 min contact time. It can be seen that the best total oil extraction efficiency had nearly 25% at solid to liquid ratio 2/15. When the amount of SBE increased, the extraction efficiency dropped continuously because the higher weight of SBE led to more adsorbed surfactant monomers on SBE. Conversely, we consider that at very low ratio of SBE loading to surfactant solution could reduce the interaction between oil and surfactant.

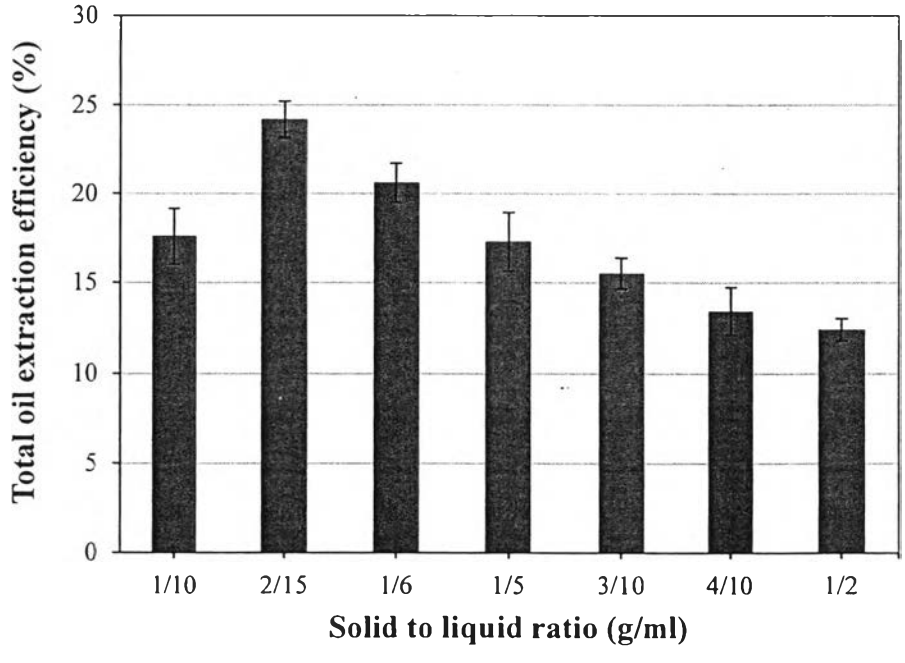

Figure 4.26 Total oil extraction efficiency versus 2.5 wt% NaCl for 1 wt% $C_{12,13}H_{25,27}$–$(PO)_8$–SO_4Na system with 1000 rpm for 20 min.

In addition, we found that the extracted oil from hexane method mainly contains solid fraction whereas oil recovered by surfactant consisted dominantly of liquid fraction, as shown in Figure 4.27. It can be clearly explained that the oil adsorbed on SBE mainly composed of vegetable fat rather than vegetable oil at room

temperature causing low total extract efficiency when using microemulsion based extraction. According to result of Do *et al.* (2014), detergency performance using anionic extended surfactant and co-surfactant reduced at temperatures below the melting points of the coconut and palm kernel oils which is semi-solid oil.

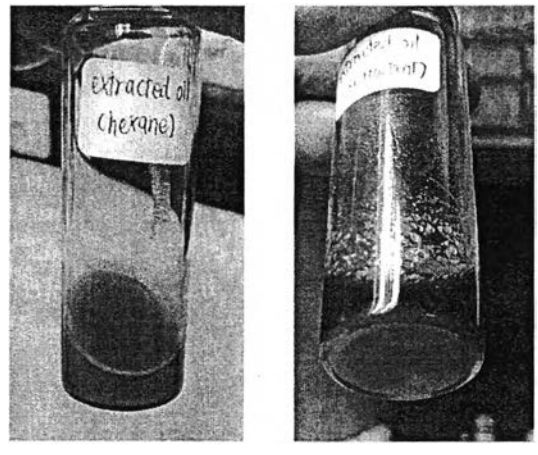

(a) (b)

Figure 4.27 Extracted oil obtained from (a) hexane extraction (b) microemulsion based extraction.

In conclusion, the appropriate surfactant system for oil extraction from SBE needs a strong interaction of head group and high hydrophobic such as anionic extended surfactant ($C_{12,13}H_{25,27}$–$(PO)_8$–SO_4Na), which consists of sulfate as a head group and PO groups as an extended tail length. This surfactant was able to interact with combination of polar and non-polar chains of vegetable oils resulting in an ultra low IFT achievement and high oil extraction efficiency. The $C_{12,13}H_{25,27}$–$(PO)_8$–SO_4Na provided the highest total oil extraction efficiency of 25% using surfactant concentration of 1 wt% at 2.5 wt% NaCl and room temperature with solid to liquid ratio 2/15, stirring 1,000 rpm and 20 min contact time. Although total oil extraction efficiency was improved to around 25% at optimum condition, this purpose method has some limitation for replacement hexane extraction because of the interaction between surfactant and absorbed oil in the form of semi-fat, which could results in lower oil removal efficiency compared with solvent extraction (hexane). However,

the oil quality between two methods would be compared. Due to small quantity of extracted oil, the scale-up extraction was then studied for evaluation of extracted oil quality, determination of the proportion of oil recovered, triglycerides analysis.

4.3 Scale-up of the Microemulsion Based Extraction

Spent bleaching earth (20g) was extracted using the optimum extraction conditions determined from the previous section (1 wt% $C_{12,13}H_{25,27}$–$(PO)_8$–SO_4Na, at 2.5 wt% NaCl, 20 min extraction time and 150 ml surfactant solution). The free oil was separated from the surfactant solution and dried at 110 °C for 24 h before weighed and transferred to transesterification for quality analysis. For residual SBE, it was dried and extracted residual oil by soxhlet extraction (hexane). The combination between amount of extracted oil by microemulsion based method and residual oil remaining in SBE compared to total oil content determined by soxhlet extraction. The mass balance was conducted to ensure that the some of oil molecules are solubilized in emulsion. In addition, the composition of oil was analyzed by weighing and evaluated as triglyceride by high performance liquid chromatography with an evaporative light scattering detector (HPLC-ELSD)

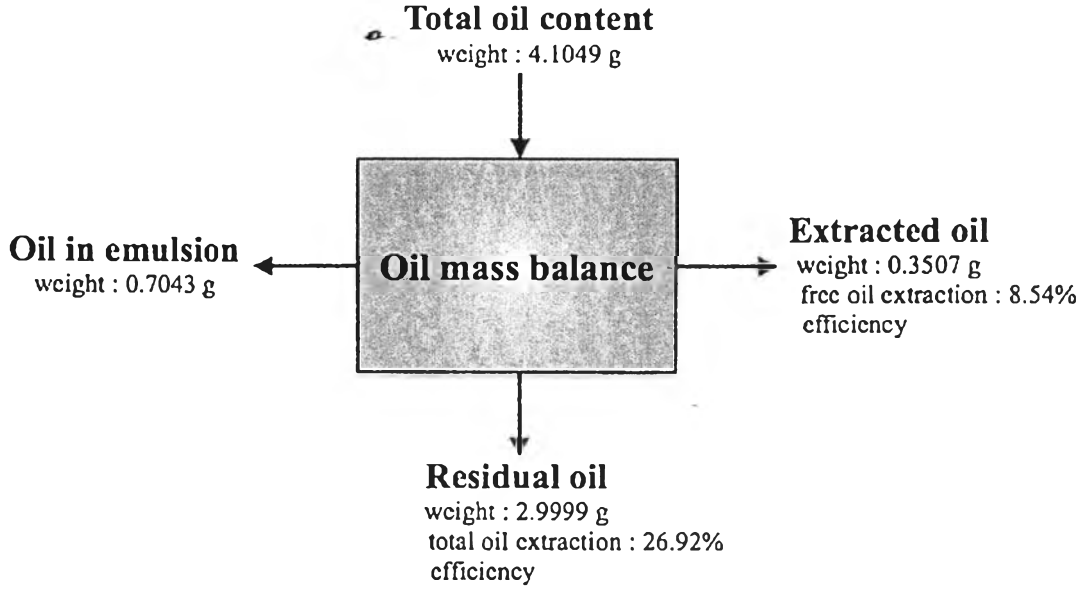

Figure 4.28 Oil mass balance of microemulsion based extraction.

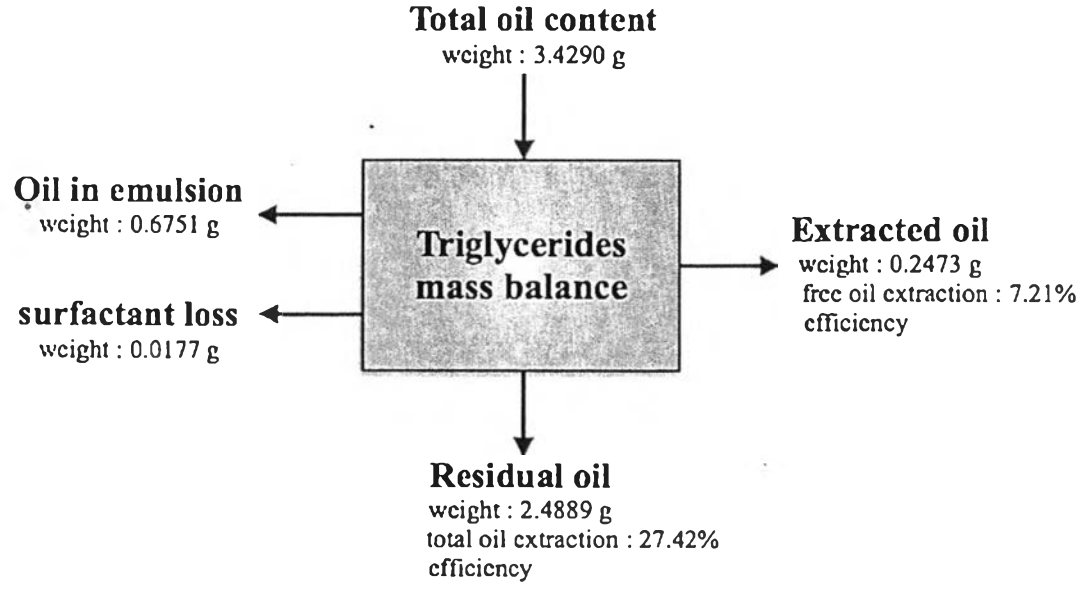

Figure 4.29 Triglycerides mass balance of microemulsion based extraction.

The mass balance of oil and triglyceride composition is illustrated in Figure 4.28 and 4.29, respectively. To start with oil mass balance, the different amount of total oil and residual oil was used to present the amount of total extracted oil which was formed in free oil and emulsion accounting for 0.3507 g and 0.7043 g, respectively. Moving to the mass balance of triglyceride composition, the small amount of extracted oil is lost from the solution about 0.0177 g. It is probably to note that these losses oil was dissolved in water during wash step of residual SBE. The comparison of free oil extraction efficiency, the proportion of free oil extraction efficiency by weighing technique (8.54%) was slightly higher than those of triglyceride composition analyzed by HPLC (7.21%). In terms of total oil extraction efficiency, both analytical methods presented a similar number, resulting in 26.92% and 27.42% for weighing and HPLC method, respectively. It is reasonable to assume that the weighing method is sufficient to evaluate the extraction efficiency for this research.

4.4 Oil Quality

The quality of extracted oil obtained from microemulsion-based extraction was evaluated and compared to that of hexane extraction. The parameter including color appearance, β-carotene, free fatty acid (FFA), surfactant and fatty acid compositions were selected for comparison. The results are summarized in Table 4.3.

Table 4.3 Comparison of extracted oil characteristics between hexane and microemulsion based extraction

Parameters	Crude palm oil	Hexane extraction	Microemulsion based extraction
Color	Orange red	Dark brown	Dark brown
β-carotene (ppm)	20.96	2.55	3.32
FFA (%)	6.75	13.30	10.50
Fatty acid composition (wt%)			
Saturated			
C12:0	0 - 0.2[a]	0.40	0.44
C14:0	0.8 - 1.3	1.29	1.24
C16:0	43.1 - 46.3	54.11	47.33
C18:0	4 - 5.5	5.09	4.92
C20:0	0.1 - 0.4	0.43	0.41
Total	48 - 53.7	61.32	54.34
Unsaturated			
C16:1	0 - 0.3	0.12	0.13
C18:1	36.7 - 40.8	32.98	37.28
C18:2	9.4 - 11.9	3.82	4.23
C18:3	0.1 - 0.4	0.08	0.10
C20:1		0.1	0.12
Total	46.2-53.4	37.1	41.86

Note: [a] Fatty acid composition of crude palm oil reported by Lusas *et al.* (2012)

4.4.1 Color and β-carotene

The color of extracted oils from visual observation is showed in Figure 4.30 and compared to crude palm oil. The appearance of extracted oil resulting from microemulsion based extraction was clearness and dark brown as the same as the oil recovered using soxhlet hexane extraction. However, these extracted oils were more dark brown in color compared with that of crude palm oil (Ramasamy, 2001)

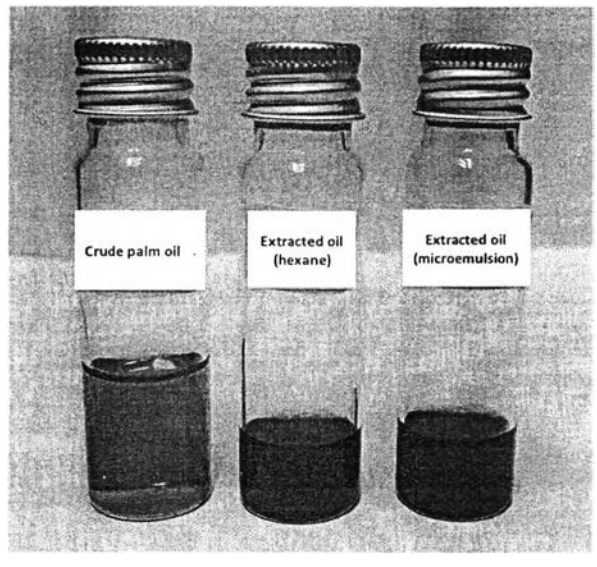

Figure 4.30 Appearance of crude palm oil and extracted oil from hexane and microemulsion based extraction.

The crude palm oil commonly contains a great amount of β-carotene, which is a colored red-orange pigment. Thus, the β-carotene composition in extracted oils was also evaluated. It can be seen from the Table 4.3 that the extracted oil from microemulsion method has slightly higher in β-carotene than that of hexane extraction and has nearly sevenfold compared to crude palm oil. The result exhibited that the surfactant structure having higher hydrocarbon chains and PO groups had more ability to interact with β-carotene structure which made of eight isoprene units and beta-rings at both ends of molecule.

4.4.2 Free Fatty Acid (FFA)

Free fatty acids were measured by direct titration with standard alkali. The FFA content in all extracted oils was higher than that of crude palm oil which composes of 6.75% FFA. The increase quantity of FFA was conducted by hydrolysis of triglycerides, which is a reaction from acid site of bleaching earth. This result was similar to the results obtained from recovery oil using solvent (Lee *et al.*, 2000). Due to a poor quality of oil described in terms of FFA value, the extracted oil obtained microemulsion has better quality than another extracted oil. However, high FFA (more than 10%) is limited in food application. Thus, these residual oils can be converted to methyl ester as biodiesel as an alternative utilization (Kheang *et al.*, 2006).

4.4.3 Fatty Acid Composition

Fatty acids are the building of a triglyceride molecule, which are the main component in vegetable oil. Fatty acid consists of a even carboxylic acid with a long aliphatic chain ranging from 4 to 22 carbons in length, which is either saturated or unsaturated. Saturated fatty acids have hydrogen atoms in theirs chain. These molecule form the fats or solid at room temperature. The unsaturated fatty acids have one or more double bonds between the individual carbon chains. These bonds can convert to a single bond by adding hydrogen atom (hydrogenation) as a result of saturated fatty acids. Therefore, the quality of extracted oil was characterized in terms of fatty acids composition. The fatty acid composition in extracted oil was converted to methyl ester through transesterification and determined by GC-FID (Lepage and Roy, 1986).

According to the Table 4.3, the total saturated fatty acids composition of extracted oil obtained hexane method (61.32%) has higher number than those of recovery oil from microemulsion based extraction (54.34%). It is obvious to note that the main component of oil adsorbed on SBE consists of solid fat and minor composition contains liquid oil at room temperature (below melting point of saturated fatty acids as shown in Table 4.4). It is a good agreement with extracted oil appearance as displayed in Figure 4.27. Arrangement of solid fat molecules is more tightly than that of liquid oil molecules. Thus, surfactant poorly interacts with the

crystalized structure of solid fats, causing low removal oil efficiency. However, the proportion of microemulsion based extraction can effectively extract liquid oil from SBE surface according to comparison the proportion of total unsaturated fatty acids between hexane and microemulsion extraction, resulting in 37.11% and 41.86%, respectively. Additionally, the quite fatty acids of extracted oil quality by alternative method are in a range of crude palm oil. Whereas, the composition of recovery oil extracted by hexane is a slight difference in palmitic (C16:0) and linoleic acid (C18:2) from crude palm oil.

Table 4.4 Fatty acids composition of palm oil and its fractions (Lusas *et al.*, 2012)

Fatty acid composition (wt%)	Common name	Melting point (°C)
Saturated		
C12:0	Lauric	44.2
C14:0	Myristic	54.4
C16:0	Palmitic	62.9
C18:0	Stearic	69.6
C20:0	Arachidic	75.4
Unsaturated		
C16:1	Palmitoleic	0.5
C18:1	Oleic	16.3
C18:2	Linoleic	-6.5
C18:3	Linolenic	-12.8
C20:1	Gadoleic	23-24

In summary, although the microemulsion based extraction has lower oil extraction efficiency than hexane method because of mainly solid fat in oil remaining on SBE, the extracted oil produced by microemulsion based extraction is similar to recovery oil obtained hexane extraction. The β-carotene content has higher and in better quality in terms of free fatty acid composition in microemulsion based

extraction as compared with another method. Thus, microemulsion based extraction can be an approach method for β-carotene extraction. In addition, this extracted oil can be a utilized as biodiesel due to high triglyceride and free fatty acid compositions (Huang and Chang, 2010) and other applications such as lubricants, grease, detergents, soap and other olechemicals.

4.5 Residual Spent Bleaching Earth

As microemulsion based extraction produced lower extraction efficiency compared to hexane extraction, this study also analyzed not only extracted oil quality but also residual SBE. The appearance and microstructure of the residual SBE was studied by visual observation, surface characterization using scanning electron microscope (SEM) and functional groups using Fourier transform infrared spectroscopy (FTIR).

4.5.1 Residual Spent Bleaching Earth Appearance

For visual observation, the image of spent bleaching earth as shown in Figure 4.31(a) had black in color and coalesce to larger size due to oil and moisture. For SBE after oil extraction process by hexane as a solvent (see Figure 4.31(c)), the appearance of residual SBE was grey in color and small size. On the other hand, the brown residual SBE from microemulsion extraction technique as presented in Figure 4.31(b) was observed. According to comparison of all appearances, the residual SBE obtained from hexane extraction was completely difference in color and size from SBE and residual SBE using microemulsion based extraction because of the residual oil. A striking point is that the color of residual SBE extracted by surfactant was lighter and darker than those of SBE and residual SBE obtained hexane, respectively. However, its size and appearance were similar to those of origin SBE. It can be concluded that microemulsion can remove partial amount of oil adsorbed on SBE leading to lower oil extraction efficiency compared to solvent extraction. However, the visual observation cannot identify for appearance in a micro scale. The SEM and FTIR technique were then investigated for microstructure and functional group observation, respectively.

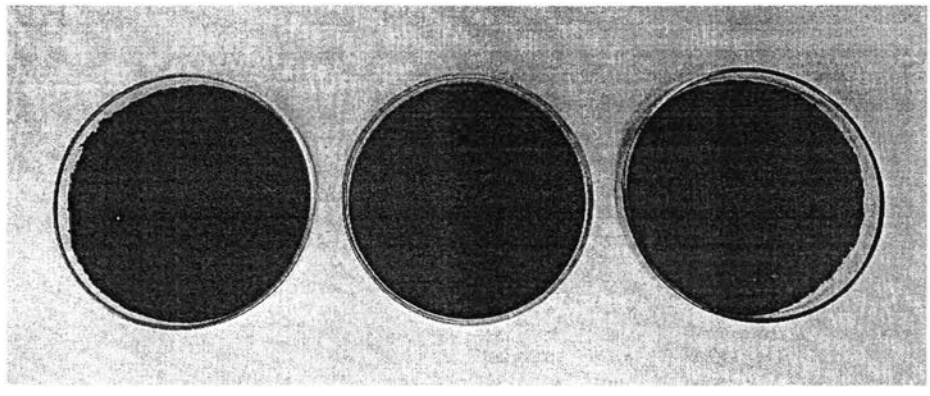

(a) (b) (c)

Figure 4.31 appearance of SBE (a), residual SBE obtained microemulsion based extraction (b) and residual SBE obtained hexane extraction (c).

4.5.2 Microstructure of Spent Bleaching Earth

The composition including oil adsorbed on SBE was characterized using SEM as illustrated in Figure 4.31(a). It can be seen that the residual SBE surface through microemulsion based extraction has slight difference from that of SBE. For microstructure of residual oil by hexane extraction in Figure 4.31(c), some component adhered on SBE surface was not observed and has the greatest change compared with SBE surface. It is assumed that some disappeared components from SBE surface may be extracted oil. Thereby, partial composition holding on SBE's surface is extracted by surfactant but other composition remained on that of surface. It is excellent suggestion that microemulsion based extraction has lower total oil extraction efficiency compared to hexane technique. However, the SBE and residual SBE were evaluated by FTIR spectroscopy in order to identify structure of oil adsorbed on SBE surface.

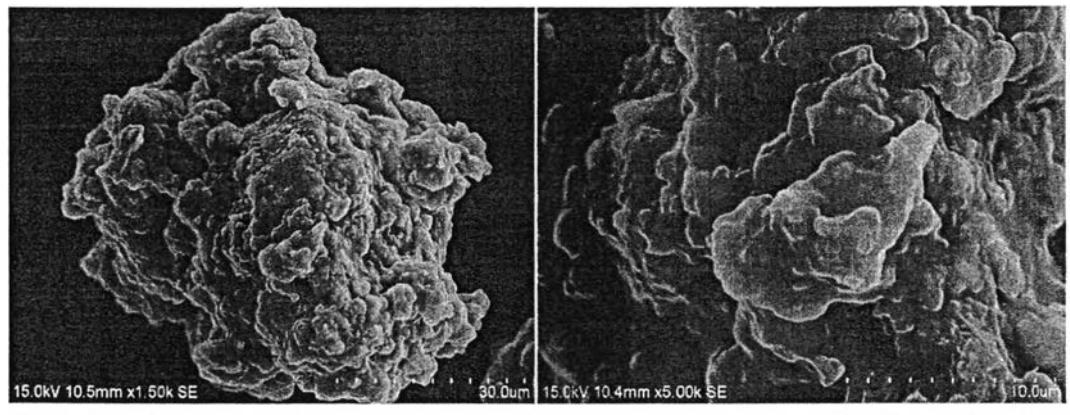

(a)

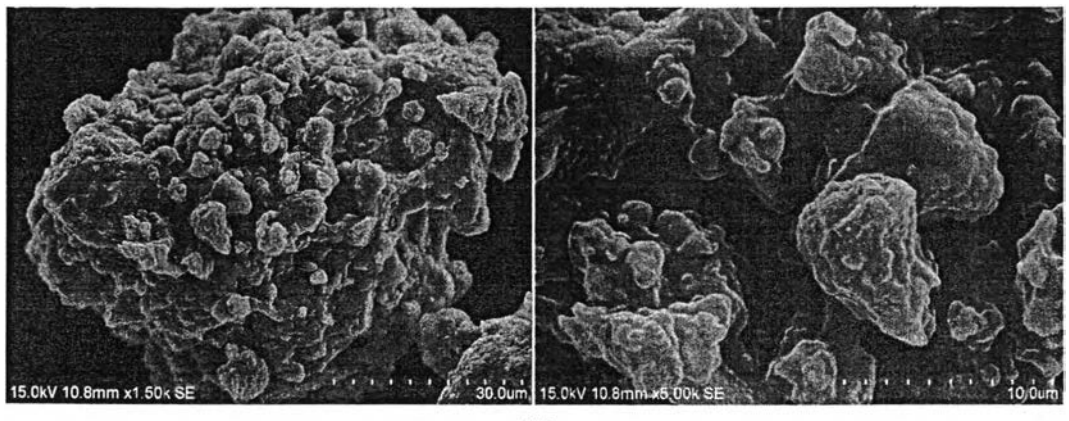

(b)

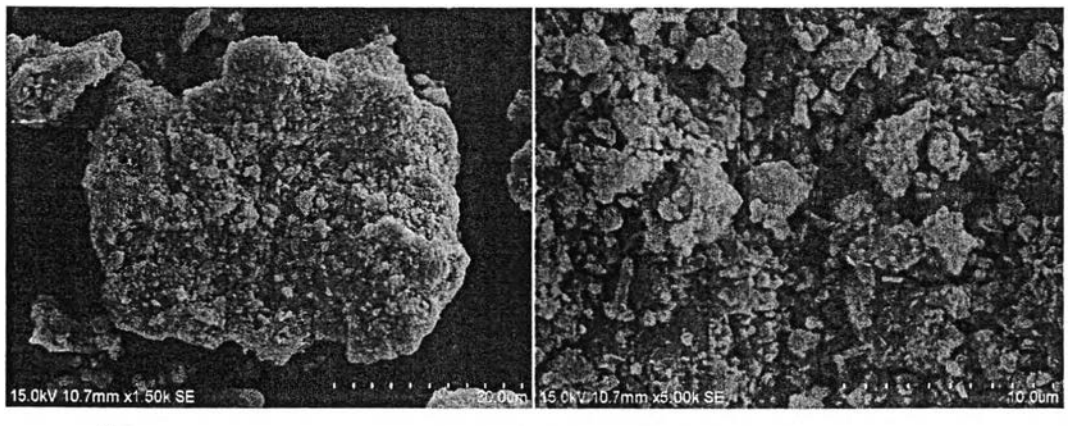

(c)

Figure 4.32 SEM images of SBE (a), residual SBE obtained from microemulsion based extraction (b) and residual SBE obtained from hexane extraction (c).

4.5.3 Functional Groups Analysis

The function group of adsorbed oil was identified using FTIR spectroscopy. The FTIR spectra of extracted oil (Figure 4.33) can be determined the function group of adsorbed oil and compare those spectra with that contains in triglyceride. The peaks at 2924 cm^{-1} and 2850 cm^{-1} assign to C-H symmetrical and asymmetrical stretching vibration of saturated carbon-carbon bond. The C=O group of triglycerides resulting a stretching vibration was observed at 1743 cm^{-1}. The peaks at 1155 and 1098 cm^{-1} correspond to stretching vibrations of the (C-O) esters group (Ullah *et al.*, 2014).

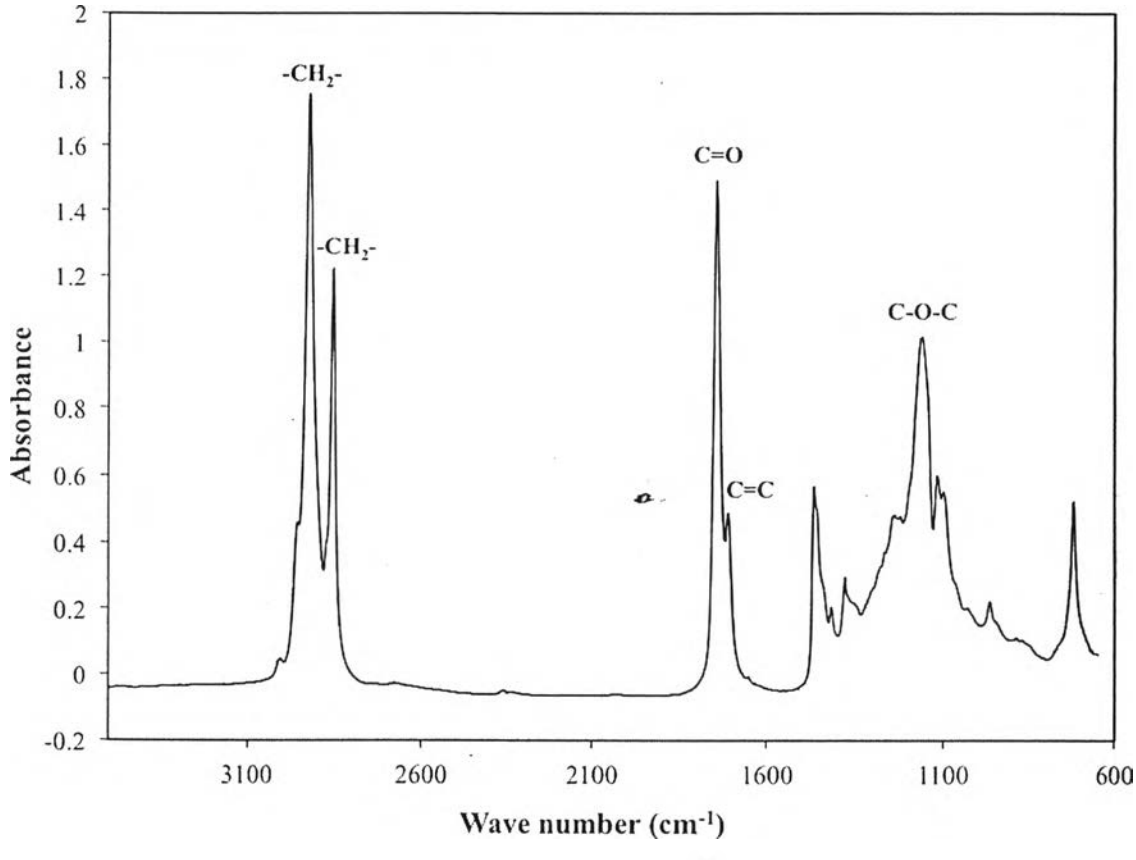

Figure 4.33 FTIR spectrum of extracted oil.

The FTIR spectra of SBE and residual SBE from microemulsion based extraction and hexane extraction were compared as shown in Figure 4.34. The absorbance of residual SBE from hexane method has a great difference while the spectrum of residual SBE using microemulsion based extraction was slightly lower than that of SBE. It is reasonable to explain that the microemulsion method has higher quantity of adsorbed oil on SBE comparing to hexane extraction method. Thus, the efficiency of proposed technique in oil extraction was not as high as hexane extraction method. This is comparable with result of oil extraction efficiency and extracted oil appearance observed in previous section.

From the results mentioned above, it can be concluded that microemulsion based extraction has less the efficiency of oil removal compared with solvent extraction due to its solubilizing efficiency with solid fat adsorbed on SBE.

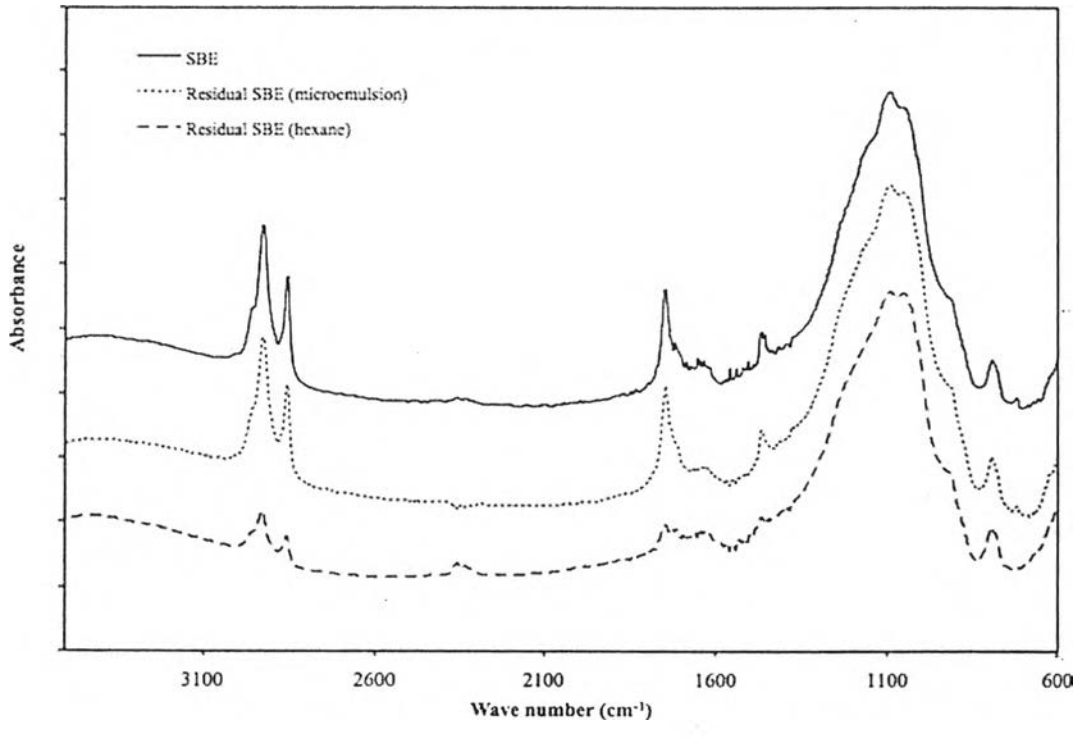

Figure 4.34 FTIR spectrum of SBE and residual SBE from microemulsion based extraction and hexane extraction.